4-2002

Development of a Data Acquisition and Analysis System

Michael V. Mores '02
Illinois Wesleyan University

Development of a Data Acquisition and Analysis System for Plasma Diagnostics

by

Michael V. Mores

Submitted to the Department of Physics
in partial fulfillment of the requirements for Research Honors

at

Illinois Wesleyan University

April 2002

Author: Michael V Mores
Department of Physics
4/30/02

Certified by:
Jeremiah Williams
Reader

Certified by: K J Detweiler
Lew Detweiler
Reader

Certified by: Narendra Jaggi 4-30-02
Narendra Jaggi
Reader

Certified by: Melyvin Jeter 5/1/02
Melyvin Jeter
Reader

Certified by:
Gabe Spalding
Reader

ABSTRACT

Plasma is the fourth and least understood state of matter. A more complete understanding of this state of matter has numerous practical applications, including fusion energy, space travel, materials synthesis, and thin film deposition. As such, there is an obvious motivation to study this state. To do this, we have constructed a radio-frequency plasma device at Illinois Wesleyan University. I have developed a data acquisition using LabVIEW software that can digitize eight analog signals, saving the data to disk for later analysis. I have also written analysis software using LabVIEW to extract meaningful information from Langmuir Probe Trace.

ACKNOWLEDGEMENTS

I would first like to thank my research advisor and colleague, Jeremiah Williams. He has assisted me in so many ways, the most important of which was helping me gain the determination to put everything I had into this project. He taught me how to continue and succeed when I felt like giving up.

Matt Highland was an incredibly supportive partner throughout the semester. It made the project much easier, knowing that we were in the project together.

I would also like to thank the professors on my Defense Panel for taking the time to read my thesis and add comments: Dr. Gabe Spalding, Dr. Narendra Jaggi, and Dr. Melvyn Jeter.

One final thanks goes out to my friends, especially those in Phi Mu Alpha, Sinfonia, who constantly cheered me on, and my loving girlfriend, Rebecca Fredericks, who will always support me in whatever I decide to do.

Table of Contents

TABLE OF FIGURES

NOMENCLATURE

Variable	Description	Units
A	Area of the Langmuir probe	m^{-2}
B	Magnetic field	Gauss
C_L	Capacitance of the L bank of capacitors	ranges between 0.02nF-0.07nF
C_T	Capacitance of the T bank of capacitors	ranges between 0.18nF-6.15nF
D	Generic plasma dimensions	m
ε_0	Permittivity of free space	$8.854*10^{-12}$ $C^2/(N*m)$
eV	Electron volt	11,600 K or $1.6 * 10^{-19}$ C
I_{es}	Electron saturation current	mA
$I_{e\,sat}$	Electron saturation current at V_S	mA
I_{is}	Ion saturation current	mA
kT_e	Electron temperature	J
L	Inductance of the antenna	mH
λ_D	Debye length	m
m_e	Mass of the electron	$9.11 * 10^{-31}$ kg
m_i	Mass of the ions	kg
n	Plasma density	m^{-3}
N_D	Number of particles in Debye Sphere	unitless
n_e	Electron number density	m^{-3}
n_i	Ion number density	m^{-3}
q	Charge on the particles (also e)	$1.6 * 10^{-19}$ C
R	Resistance of the antenna	Ω
τ	Mean time between collisions in a plasma	sec
v	Velocity of the particles	m/s^2
V_b	Potential given by B-Dot probe	V
V_P	Probe potential	V

V_s	Plasma space potential	V
ω	Frequency in the matching circuit	sec^{-1}
ω_p	Frequency of plasma oscillations	sec^{-1}
Z	Impedance of the antenna	Ω

Chapter 1

Introduction

If one were asked to define what plasma is, one might say that a plasma is an ionized gas that usually exists at only extremely high temperatures. A more accurate, and rigorous, definition is offered by Chen: "...a quasi-neutral gas of charged and neutral particles which exhibits collective behavior."[1] Quasi-neutrality refers to a plasma in which the number of ions and electrons to be on the same order of magnitude. A more detailed definition is given in Section 1.1. By equation 1, we see that in plasmas,

$$n_i \approx n_e \approx n \tag{1}$$

Collective behavior, on the other hand, refers to the local behavior of the plasma is determined by long range coulombic forces, rather than local interactions, such as in a gas. While both are essential in defining a plasma, there are three criteria that allow one to quantify the plasma state.

1.1 Plasma Characteristics

Plasmas are a quasi-neutral collection of free charged particles. As a result, any charge build up within the plasma will be quickly be "sheltered" by charges of opposite polarity. Likewise, plasmas have the ability to screen applied electric fields. For example, if one was to insert an electrode into a plasma and apply a bias, charges from within the plasma would naturally congregate to the electrode, shielding the remainder of the plasma from the applied potential. This process is known as Debye Shielding. The thickness of the charged "cloud" is known as the Debye length and depends on a number of factors, including the thermal energy of the system, measured by the temperature, the electron density, and the ion density. The Debye

measurement of the sphere of influence that a given charge has. For a plasma to be quasi-neutral, the majority of the plasma must be free of large electric potentials and fields. As such, the Debye length, must be much smaller than the size of the plasma, D, and is given by Equation (2):

$$\lambda_D = \left(\frac{\varepsilon_0 k T_e}{n_e e^2} \right)^{\frac{1}{2}} \tag{2}$$

In order for the Debye length to have significance, the number of particles in a Debye sphere, Equation (3), must be much greater than 1. Physically, for Debye shielding to be statistically meaningful, the plasma must have a large number of particles in the Debye sphere.

$$N_D = n \frac{4}{3} \pi \lambda_D^{\ 3} \tag{3}$$

The third, and final, requirement for defining a plasma deals with collisions. In order to satisfy the condition of collective behavior, these ionized particles should not have frequent collisions with neutral particles. If this is not so, then the ionized gas would be controlled by these collisions rather by electromagnetic forces. To ensure the behavior is not governed by collisions, we require that the product of the frequency of typical plasma oscillations and the mean time between collisions with neutral atoms is less than one. Thus, an ionized gas must satisfy the following criteria in order to be classified as a plasma:

$$\begin{aligned} &\lambda_D << D \\ &N_D >> 1 \\ &\omega_\pi \tau > 1 \end{aligned} \tag{4}$$

1.2 Objectives

It is generally accepted that 99% of the matter of the universe exists in the plasma state, due to the composition of stars and interplanetary nebulae.[2] Some examples of plasmas include lightening, fluorescent light bulbs and other gas-discharge tubes, and extremely hot flames. Figure 1 depicts a variety of plasmas, as a function of density and temperature.[3] Unlike the other states

Figure 1 depicts a variety of plasmas, as a function of density and temperature.[3] Unlike the other states of matter, plasmas exhibit a tremendous range of temperatures and densities. Plasma density ranges from 10^6 to 10^{34} m^{-3}, while their temperature ranges over several orders of magnitude from 0.1 to 10^6 eV.

Despite the natural abundance of plasmas in the universe, this fourth state is not well understood. While plasma physics has existed for over 80 years, a solid theoretical understanding has not yet been achieved because plasmas behave in a highly non-linear fashion. As such, experimental and numerical studies are key mechanisms in developing an understanding of the rich underlying physics.

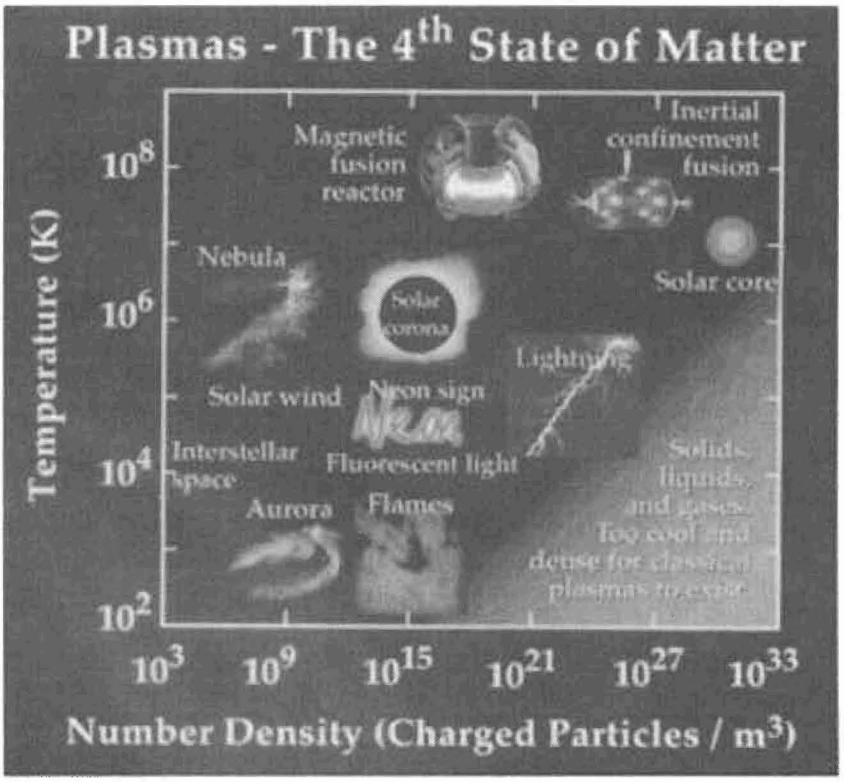

Figure 1 – A few common examples of plasmas, with related temperatures and densities

There are many practical applications that would benefit from a more solid understanding more about this state of matter, including fusion as an alternative energy source. Fusion energy is the cleanest energy form to date, reducing for need to burn fossil fuels. Deep space propulsion systems are another key area that is being studied.[4] This can be used as an inexpensive and efficient method of travel. Other areas include materials synthesis and etching, and semi-

conductor manufacturing. However, a deeper theoretical understanding of plasma physics is essential in aiding all of these areas.

In order to study this state of matter in a laboratory setting, we have begun construction of a radiofrequency plasma device at Illinois Wesleyan University. In this thesis, I provide details about the plasma chamber and the related diagnostics, as well as the focus of my thesis: the data acquisition and analysis systems. The following is an outline of this thesis:

- Chapter Two describes the experimental setup, including:
  - the plasma chamber
  - the vacuum system, and
  - diagnostic tools
- Chapter Three describes
  - the data acquisition system
  - analysis software, and
  - simulated test results with discussion
- Chapter Four will consist of
  - conclusions
  - future work, and
  - recommendations

Chapter Two

Experimental Setup, Diagnostics, and Procedures

In order to study plasmas in a laboratory setting, we have constructed a plasma device that consists of a plasma chamber, vacuum system, and the necessary diagnostics. This chapter will discuss the experimental setup, as seen in Figure 2, and the diagnostic tools that will be used.

2.1 Plasma Chamber

The plasma chamber is a steel cylinder, with a diameter of 36 cm and a length of 61 cm. An attached bell jar measures 19 cm with a diameter of about 18 cm. The chamber has an approximate volume of 6.37×10^{-2} m^3.

To create a plasma with our power capabilities, we need an operating pressure of 10^{-3} to 10^{-4} Torr.[5] A base pressure of 10^{-6} Torr is desired to ensure the purity of the gas being used. The chamber is evacuated by means of a mechanical roughing pump and a diffusion pump. To monitor the pressure, a wide variety of vacuum gauges have been used, including the Thermocouple (1-10^{-3} Torr), Pirani gauge (1 to10^{-3} Torr), Ionization gauge (10^{-3} to 10^{-9} Torr), and the Penning gauge (10^{-2} to 10^{-6} Torr). Currently, the chamber can reach a pressure of 5 mTorr.

2.2 Plasma Source

The plasma will be created using a helicon source, first used by Rod Boswell in the late 1960s at Flinders University.[6] This type of source has been used extensively in the semiconductor industry because of a high coupling efficiency between the antenna and the

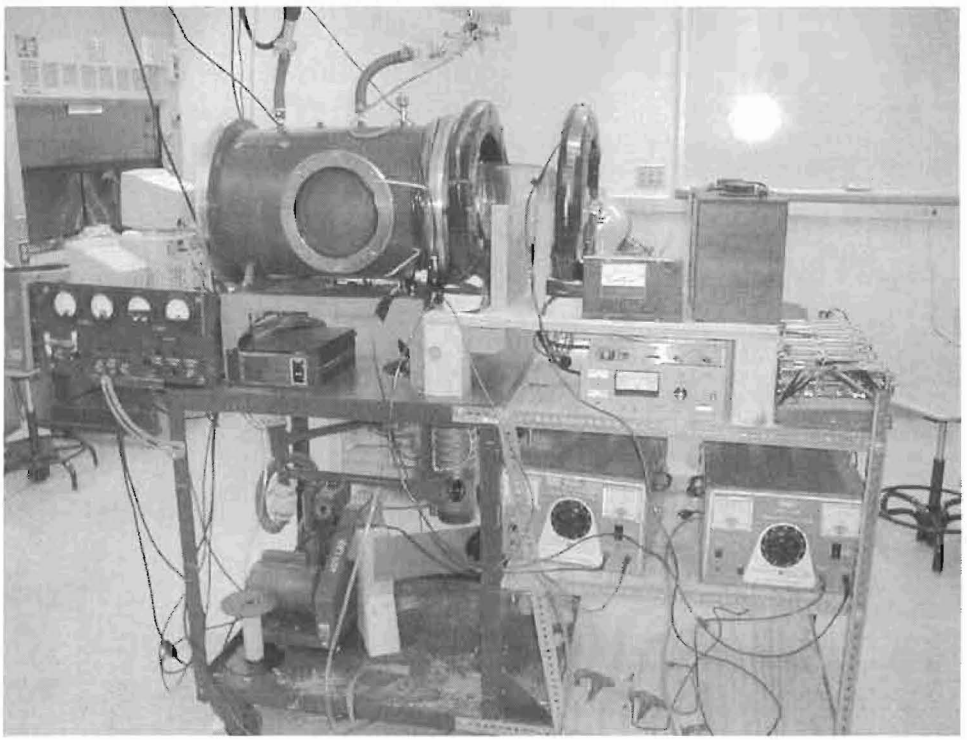

(a)

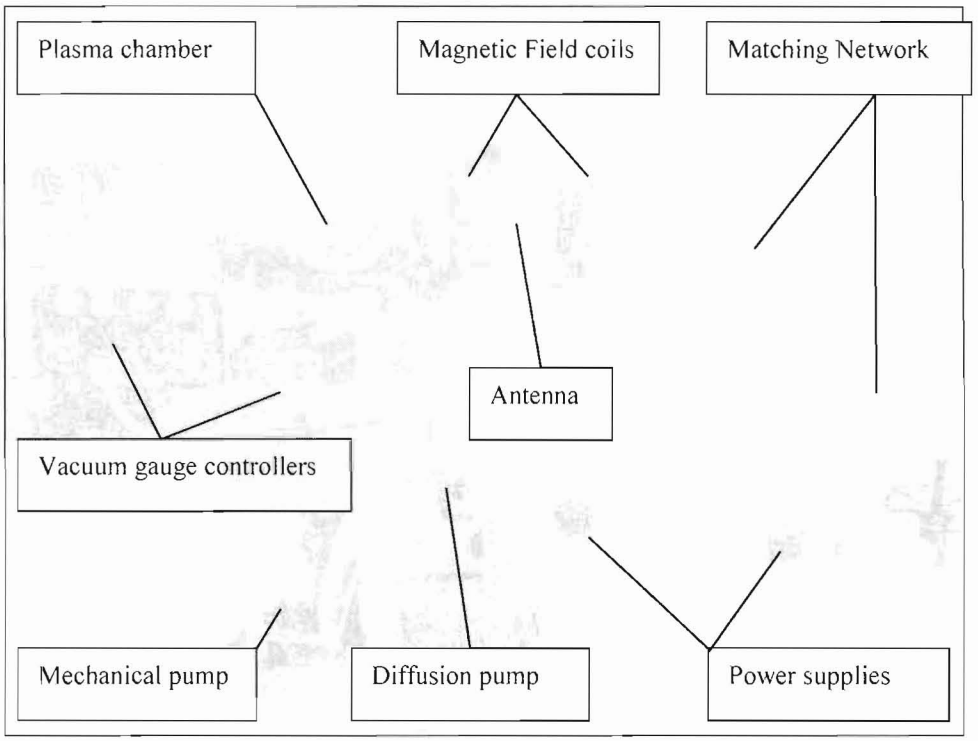

(b)

Figure 2 – (a) a photograph of the plasma device, and (b) is a legend to the device parts

plasma, which gives rise to high density plasmas at modest input powers. Recently, it has gained prominence in basic plasma physics, where it simulates the edge environment of a tokamak in magnetic fusion device and aids in the development of space plasma thrusters.

Our RF source provides up to 300W of power to a Nagoya Type III antenna, which is used to launch a helicon wave. The antenna has a resistance of 0.18 Ω and an impedance of 6 μH. This leads to an antenna impedance of Z_{ant} = 100 Ω at a typical frequency of 13.57 MHz. Due to an impedance mismatch between the source (Z_{source} = 50 Ω) and the antenna, a matching network was designed to maximize the power transfer to the antenna. The schematic for the source is seen in Figure 3.

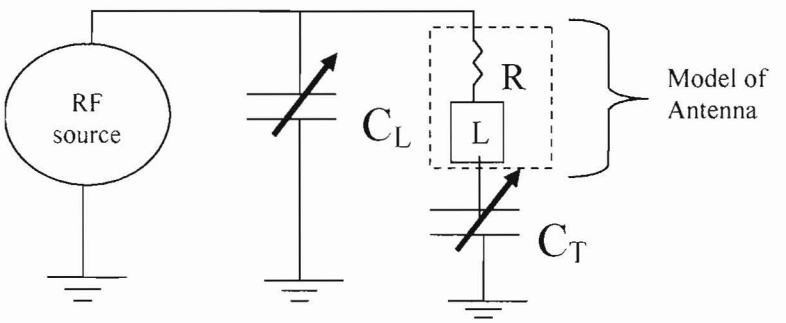

Figure 3 – A schematic for the source and matching circuit, where C_L and C_T are variable capacitors to match impedances. The antenna is modeled as an inductor and resistor in series.

The source and antenna impedances match when the load and tuning capacitors are given by Equations (5) and (6), respectively.

$$C_L = \frac{1}{\omega\sqrt{RZ}} \tag{5}$$

$$C_T = \frac{1}{\omega^2 L - \omega\sqrt{RZ}} \tag{6}$$

Currently, C_L and C_T are banks of air filled variables with ranges between 0.02nF-0.07nF and 0.18nF-6.15nF, respectively, which allows matching for frequencies greater than 8 MHz.

A helicon wave is launched by a Nagoya Type III antenna, as seen in Figure 4. The antenna was constructed from 0.24mm copper sheeting, and was selected for its simple design and high efficiency.

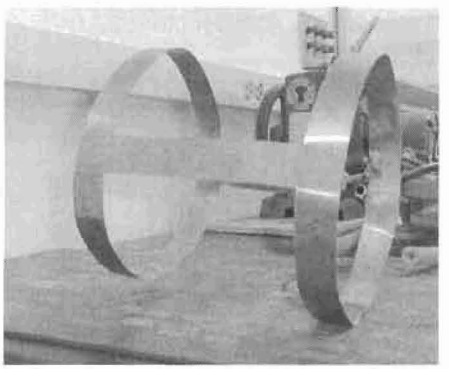

Figure 4 – The Nagoya Type III antenna that will be used with the plasma device

Since helicon waves can only propagate in a magnetized medium, the source must be located in a region of a magnetic field. This field is generated by a pair of concentric coils with 110 turns of 10 and 8 AWG wire wrapped on 18'' iron rings. These coils are capable of carrying up to 20A constant current, and create a fairly uniform magnetic fields of up to 75 Gauss. From the literature, this source should be capable of producing a plasma density in the range of 10^9 and 10^{14} m^{-3}. [7]

2.3 Diagnostics

In order to understand and model what is actually happening inside our plasma, we are interested in measuring a few parameters, mainly kT_e, V_s, and n_e, which can be found by using the Langmuir Probe. The B-Dot probe will be used to measure fluctuations in the magnetic field inside the plasma chamber.

2.3.1 Langmuir Probe

In 1924, Irving Langmuir invented a diagnostic method to measure the temperature, density, and plasma space potential using a thermionic probe, now called a Langmuir probe.[8] A schematic of this probe can be seen in Figure 5.

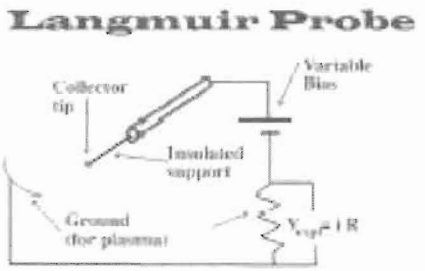

Figure 5 – Schematic of the Langmuir probe [9]

The Langmuir probe is a small metal tip that is inserted into a plasma. This tip can be a disk, a sphere, or a cylinder. Typically, these probes have a surface area of around 10^{-6} m^2. By applying a bias to the probe, one will collect particles from the velocity distribution function of each species present in the plasma with enough energy to overcome the established potential The collected charges are then measured as a current, given by Equation (7).

$$I = A\sum_i n_i q_i \bar{v}_i \tag{7}$$

where the summation is over the various species in the plasma. The average velocity in Equation (7) can be found by taking the first moment of the velocity distribution function:

$$\bar{v}_i = \frac{1}{n}\int v f_i(\vec{v}) d\vec{v} \tag{8}$$

When the probe is placed in the yz plane, a particle will collide with the probe and give rise to a current only if it has some v_x component of velocity. Thus, the current to the probe does not depend on v_y or v_z. By combining Equations (7) and (8), the current in the *x*-direction will be:

$$I = nqA\int_{v_{min}}^{\infty} v_x f(v_x) dv_x \tag{9}$$

The Langmuir probe only collects those particles with enough kinetic energy to overcome the potential established by the probe's bias.

$$qV = \frac{1}{2}mv^2 \tag{10}$$

Taking the derivative with respect to the velocity allows us to change our integration variable.

$$d(qV) = mvdv \tag{11}$$

Equation (9) can be rewritten as:

$$I = \frac{nqA}{m_e} \int_{qV}^{\infty} f(qV) d(qV) \tag{12}$$

By increasing the probe bias from a sufficiently negative value to a sufficiently positive value, one can measure the entire velocity distribution function of every species in the plasma. By taking the derivative of the measured current with respect to the probe bias, we can extract the distribution function.

$$\frac{dI}{d(qV)} \propto f(qv) \tag{13}$$

Due to collisions within the plasma, the plasma's velocity distribution function will naturally move towards a Maxwellian distribution, in the form of Equation (14).

$$f_e(\vec{v}) = n\left(\frac{2\pi kT_e}{m_e}\right)^{-3/2} \exp\left(\frac{-\frac{1}{2}m_e|\vec{v}|^2}{kT_e}\right) \tag{14}$$

By combining Equations (9) and (14), we get the current due to particles moving in the x-direction:

$$I(\vec{v}) = nqA \int_{v_{min}}^{\infty} dv_x v_x \left(\frac{2\pi kT_e}{m_e}\right)^{-3/2} \exp\left(\frac{-\frac{1}{2}m_e|\vec{v}|^2}{kT_e}\right) \tag{15}$$

When there is a negative bias is applied to the probe, the current reaches what is known as the ion saturation current. It is as this point that all of the ions near the probe are collected. In order to find the saturation current, the tip voltage must repel the electrons. This can be modeled by:

$$eV = kT_e \tag{16}$$

We can then write the ion saturation current as:

$$I_{is} = neA\left(\frac{2kT_e}{m_i}\right)^{\frac{1}{2}} \tag{17}$$

As the bias becomes increasingly positive, the probe current is due to the ion current as well as the current due to high energy electrons that are collected.

$$I(v) = I_{is} - neA\int_{v_{min}}^{\infty} dv_x v_x \left(\frac{2\pi kT_e}{m_e}\right)^{\frac{-1}{2}} \exp\left(\frac{-\frac{1}{2}m_e v_x^{\,2}}{kT_e}\right) \tag{18}$$

By combining Equations (12) and (18) and integrating, we get:

$$I(v) = I_{is} - neA\left(\frac{kT_e}{2\pi m_e}\right)^{\frac{1}{2}} \exp\left(\frac{eV}{kT_e}\right) \tag{19}$$

This equation shows that the probe current increases exponentially. This continues until the probe voltage is equal to the plasma space potential ($V = V_p - V_s = 0$). The plasma space potential is defined as the potential of the plasma with respect to the chamber potential. At this point, the probe potential is at the same potential as the plasma, and the probe is measuring the entire distribution function in the immediate region of the probe, i.e. – the probe has collected the entire distribution function within the specified Debye length. As the bias increases, the probe will begin collecting particles within a larger radius because the increased probe potential increases the Debye length. In this region, the measured current is due only to the electrons.

$$I_{es} = -neA\left(\frac{kT_e}{2\pi m_e}\right)^{\frac{1}{2}} \tag{20}$$

By understanding Equations (17), (19), and (20), we can create a graph of the current as a function of the probe potential for the three different regions. Figure 6 shows a sample Langmuir Probe Trace for a plasma having a Maxwellian distribution. In Region A, only electrons contribute to the measured current. In this region, the current increases linearly with the positive bias, as seen in Equation (20). In Region B, both the ions and the electrons contribute to the

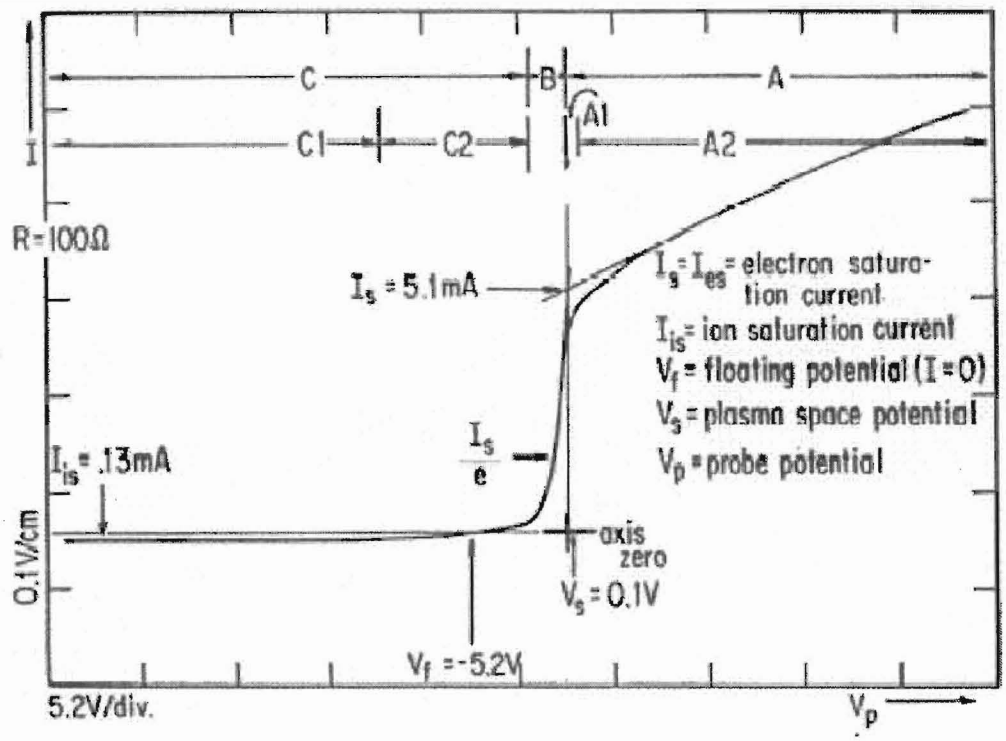

Figure 6 – A graph depicting a Langmuir Probe Trace for particles with a Maxwellian distribution. [9] This plots the current as a function of the probe potential.

measured current, as modeled by Equation (19). The electrons current is more significant than the ion current, due to a higher electron mobility. The current increases exponentially with the increasing potential of the probe. If the curve in region B is not exponential, then the velocity distribution is not Maxwellian. In Region C, only the ions contribute to the measured current, as stated in Equation (17). The current increases slowly with increasing negative potential on the probe. This will be measured as a negative current, due to the ion motion.

In order to extract the plasma parameters, we need to consider the exponential region of the Langmuir trace (Region B). By taking the natural log of Equation (19), and differentiating with respect to the probe bias, we can find the electron temperature (Equation (21)), which is the inverse of the curvature.

$$\frac{d\ln|(I)|}{dV} = \frac{e}{kT_e} \tag{21}$$

From this value, the electron density can be computed using Equation (22).

$$n_e = \frac{I_{esat}}{Ae\left(\frac{kT_e}{2\pi\, m_e}\right)^{\frac{1}{2}}} \tag{22}$$

2.3.2 B-Dot Probe

The B-Dot probe consists of a metal wire wrapped in a series of loops around some insulator, as seen in Figure 7. When the wire is inserted into a changing magnetic field, an εmf is induced by Faraday's Law:

$$V_b = nA\frac{\partial B}{\partial t} \tag{23}$$

(a)

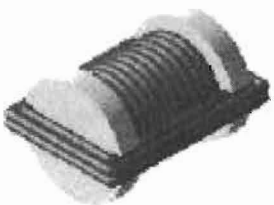

(b)

Figure 7 – (a) is a picture of the radial coil, and (b) is a picture of the θ coil [10]

Integrating the induced voltage with respect to time allows one to reconstruct the magnetic fields. This can be done through hardware, using an integrator circuit, as seen in Figure 8.

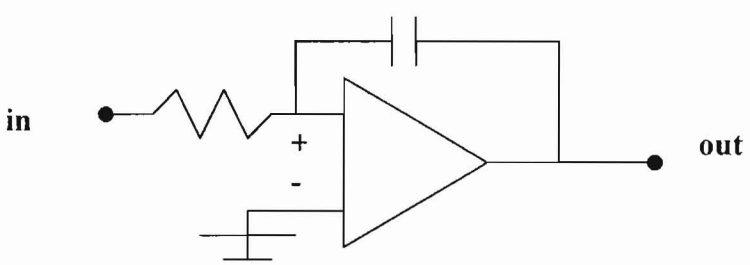

Figure 8 – An integrator circuit

Chapter 3

Data Reduction, Analysis, and Discussion of Results

The diagnostics discussed in Chapter 2 require that a voltage be read. In the case of a Langmuir Probe, the probe bias and the probe current across a resistor are measured. In the case of the B-Dot probe, we will measure a voltage proportional to the magnetic fluctuation. In order for us to analyze this data after acquisition, it must be digitized for later analysis.

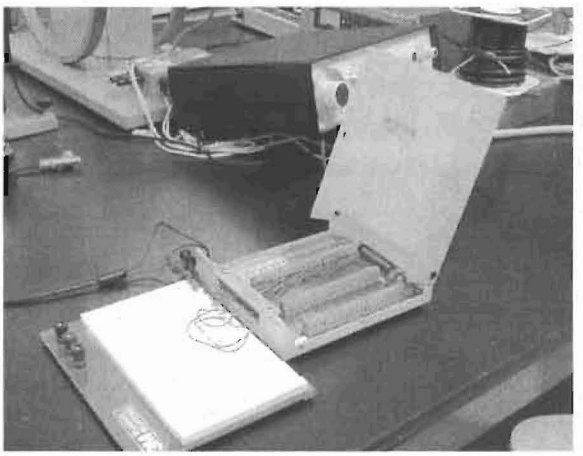

Figure 9 – The interface box used to connect the signal(s) to the DAQ card.

3.1 Data Acquisition

To digitize the analog signals from our diagnostics, the National Instruments multifunction I/O card model number 6052E was used. This 16 bit resolution data acquisition (DAQ) card is capable of recording eight differential analog inputs at a time, with a maximum sampling rate of 333 k samples per second in the range of ± 10 Volts. This sampling rate is proportional to the number of channels being used. For example, if all eight channels are being used, the sampling rate drops to about 41,000 samples/sec per channel. The specification sheet can be located in the Appendix. An interface box, as seen in Figure 9, was used to connect the diagnostics to the DAQ card.

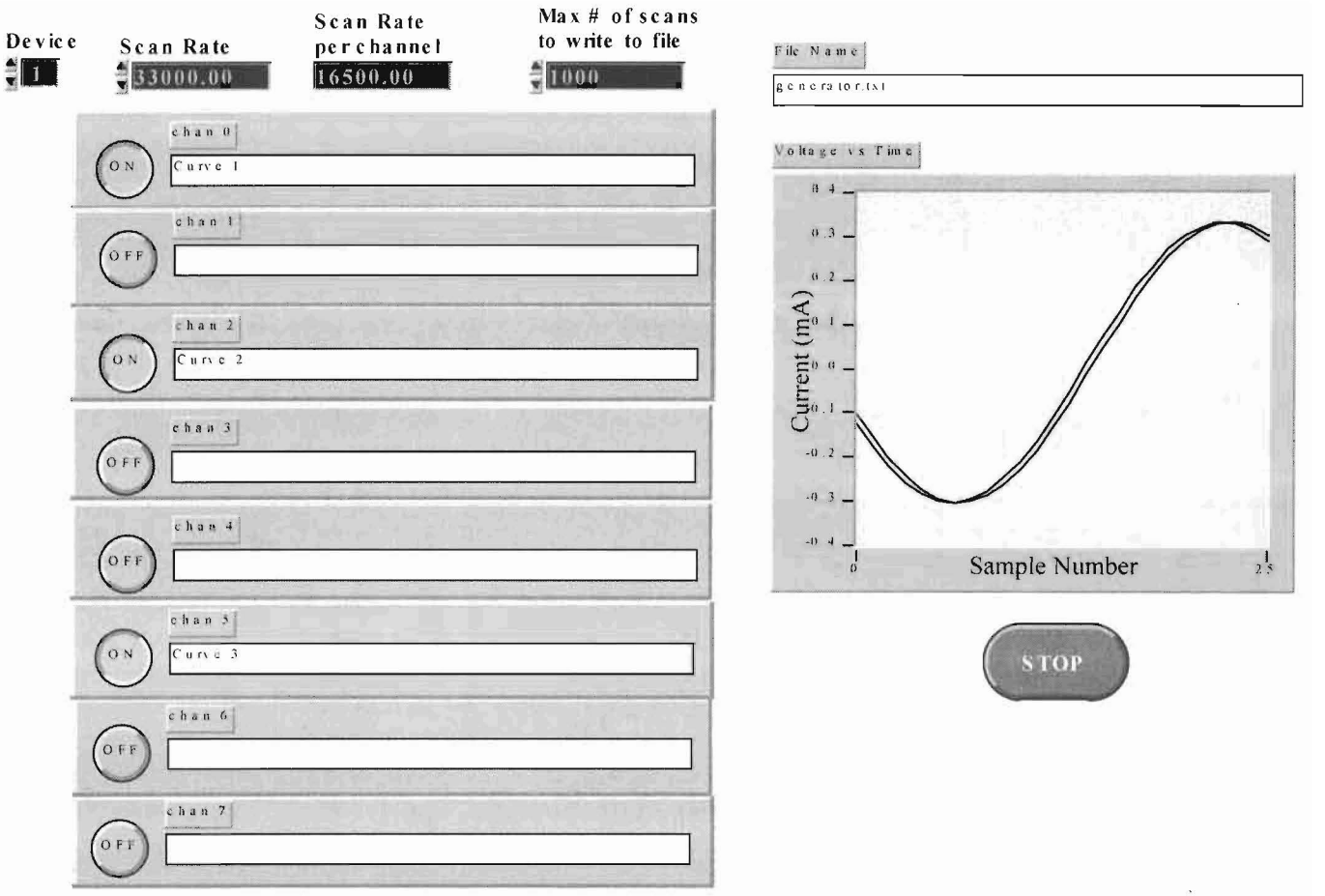

Figure 10 – This is the front panel of a LabVIEW program that I wrote showing a digitized 1 KHz sine wave trace from a function generator. In this case, I specified the max scan rate of three channels, with 1000 samples.

A program was written in LabVIEW to control the DAQ card and save the measured data to disk. The program can be found in the Appendix. Figure 10 shows the front panel, through which the user can control the DAQ card and the data acquisition process.

As seen in Figure 10, the user has control over all aspects of the data acquisition process. Beginning at the top left-hand side of the figure, the user can first choose which device they want to acquire data on, assuming they have more than one DAQ card installed. The user can input the maximum scan frequency, which is then divided among the chosen channels, and the scan rate per channel is displayed. The maximum number of scans to take on each channel can also be specified by the user. The user selects the channels to save to disk using the ON/OFF buttons to the left of the channels. By entering a channel header, the user can add comments on the channels

that are being used as the first row in the tab-delimited text file that this data is saved to. The user specifies the file by imputing the file name at the top of the program.

In case the program needs to be stopped before it has finished, there is a STOP button that can be used to halt acquisition. The data is displayed graphically on the right-hand side, so the user can see the plots. In this case, a function generator with a 1 KHz signal is being processed, with a scan rate of 33,000 scans/sec. This program has been tested extensively, and works as described. Figure 11 shows part of the file saved to disk using the setup pictured in Figure10.

Curve 1	Curve 2	Curve 3
-0.101929	-0.126343	-0.148343
-0.156555	-0.178528	-0.19528
-0.204163	-0.222473	-0.23574
-0.244141	-0.258179	-0.27496
-0.274658	-0.284119	-0.30596
-0.29481	-0.299377	-0.29541
-0.30365	-0.304565	-0.30358
-0.30092	-0.296326	-0.28457
-0.287781	-0.278625	-0.26958
-0.263367	-0.249023	-0.22487
-0.228577	-0.210571	-0.20258
-0.184937	-0.163879	-0.15014
-0.133972	-0.110474	-0.10015
-0.077515	-0.05188	-0.03542

Figure 11 – Sample table of values from the data acquisition program, as shown in Figure 10.

3.2 Langmuir Probe Trace Analysis System

A second program was written in LabVIEW to extract the plasma parameters from a Langmuir Probe Trace, such as the trace seen in Figure 6. Since an actual Langmuir Probe was not available, a program was written to generate the LPT to test the analysis software. Region C in Figure 6 was neglected as it does not contain any relevant information at this time. White noise was then added to simulate electronic noise that exists in the laboratory environment. To analyze this simulated trace, the noise in the signal was reduced using a median fit. A Spline fit was performed to extract the desired number of data points for analysis. Plasma parameters are then extracted using the methods described in Section 2.3.1. This procedure can be seen in Figure 12. The program code can be found in the Appendix.

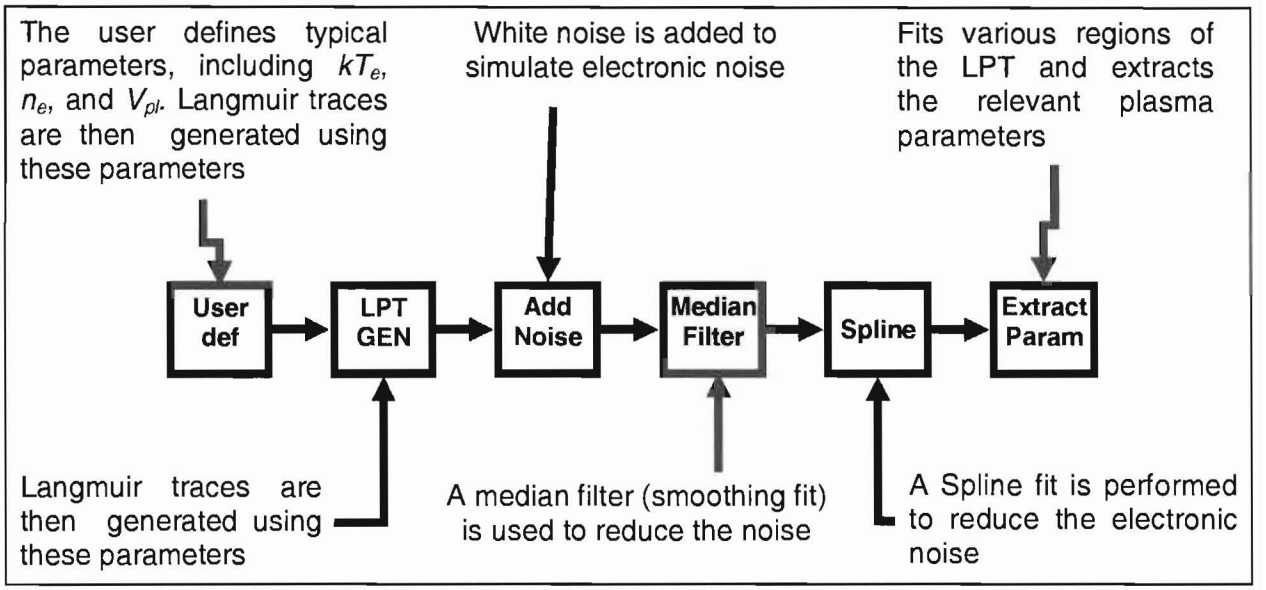

Figure 12 – The Langmuir Probe Analysis System, complete with LPT generator, noise adder, median filter, Split fit, and parameter extractor.

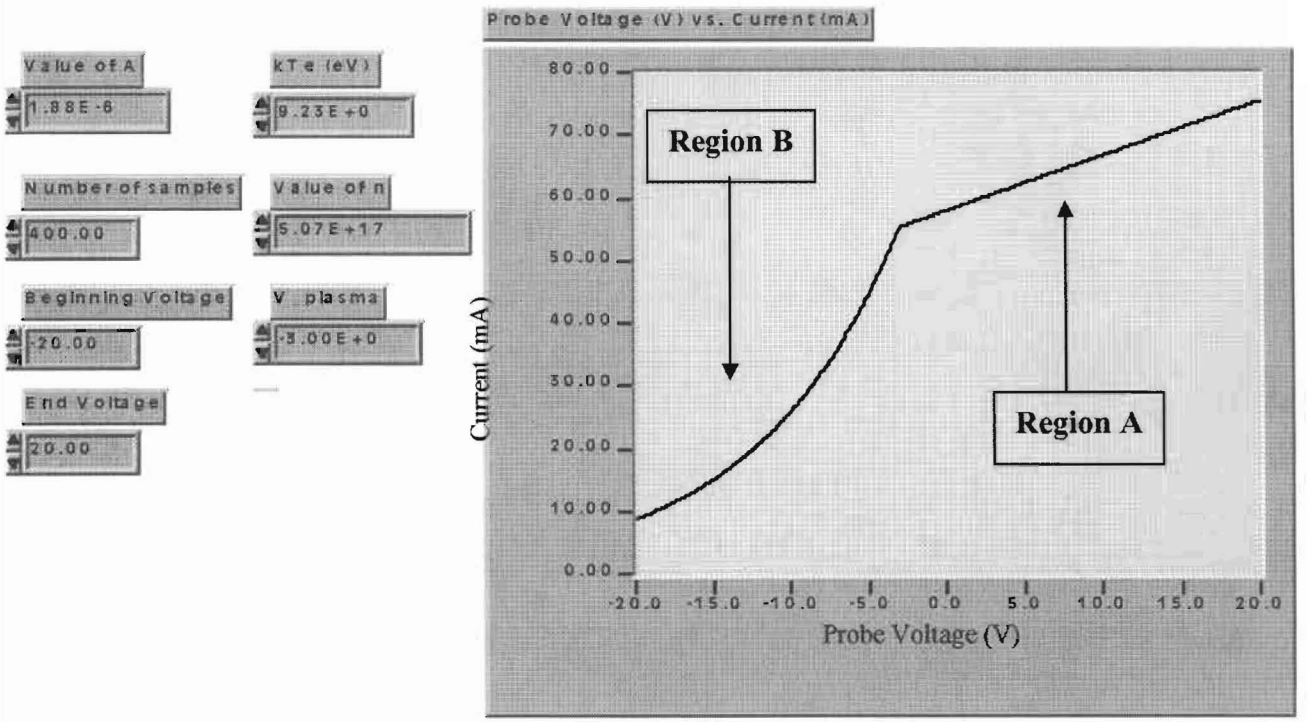

Figure 13 – Sample Langmuir Probe Trace given the values specified on the left-hand side.

3.2.1 Langmuir Probe Trace Generator

In order to test the analysis program, a program was written to simulate the relevant areas of a Langmuir trace, based on the user defined parameters: electron density, electron temperature, probe area, plasma space potential, the sweep voltage range, and the number of data points in the simulated trace. Figure 13 shows a simulated Langmuir Probe Trace, using the parameters depicted on the left-hand side. In this figure, Regions B and A refer to the exponential and linear regions of an actual Langmuir trace, respectively, as in Figure 6.

3.2.2 Noise Adder

In order to make the simulated Langmuir trace more realistic, a small amount of white noise was added to simulate electronic noise. The user defines the amplitude of desired noise, allowing one to examine the robustness of the analysis software. Figure 14 shows the LPT from Figure 13 with noise added. The amplitude of the noise was ±5.

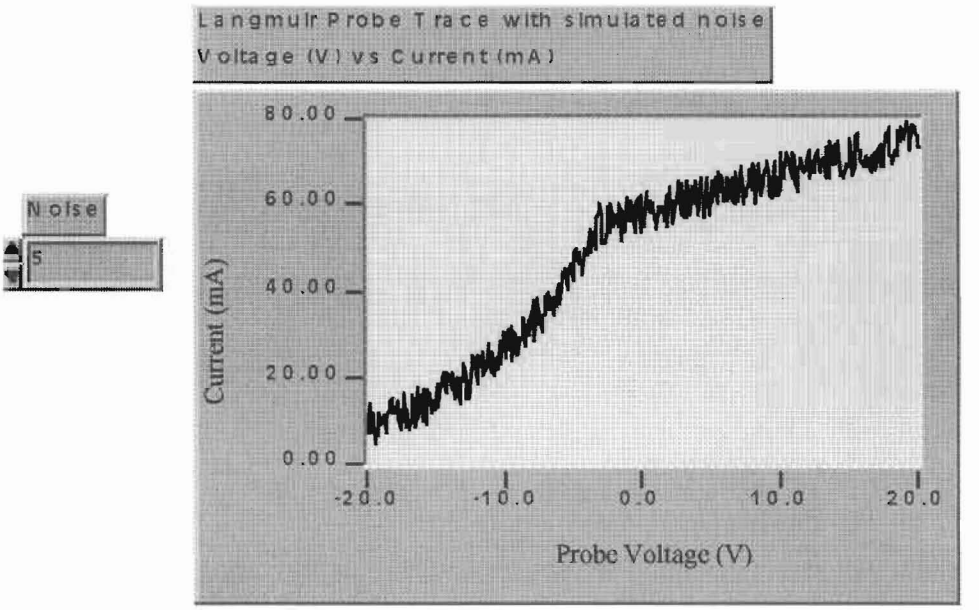

Figure 14 – Simulated Langmuir Trace from Figure 13 with a noise amplitude of ± 5

3.2.3 Data Analysis – Noise Reduction

To extract parameters from a Langmuir trace, the first step involves reducing the noise that is present. Three methods of noise reduction have been tested.

The first method involved smoothing the data using a median filter. This fit approximates the curve with an input rank, *r*, value from the user. This works by approximating each element of the curve with relation to *r* number of data points on each side of the element. This introduces some error at the beginning and the end of the Langmuir Trace, due to the fit's inability to approximate data points at the ends. In order to avoid the approximation problem from the median filter, the first 10 and last 50 data points are ignored in the graph. Figure 15 shows the data smoothed using a median filter with a rank of 10, as shown by the thick line.

The second method used to reduce the signal noise was a low pass filter. In this method, the curve filtered by the user specifying the cutoff frequency. This fit will keep the frequencies lower than the cutoff frequency and remove the higher frequencies. In this case, we kept the frequencies lower than 25 Hz. The filter order refers to an output array of size two. While this method did work, the output data was positively biased with relation to the input data. This was not surprising, since white noise was added. It is possible that the noise could be Gaussian, in which case this method would be more effective.

The final method used to reduce the signal noise was to perform a Fourier transform on the probe data. The region of the spectrum that contains the signal is then transformed back into real space, thereby reducing the noise. At the present time, we have been unable to get the technique to work correctly.

After a number of tests, it was determined that although the smooth fit and the low pass filter both reduce the amount of noise in the signal, the smooth fit performs better with white noise. For this reason, the smooth fit was chosen.

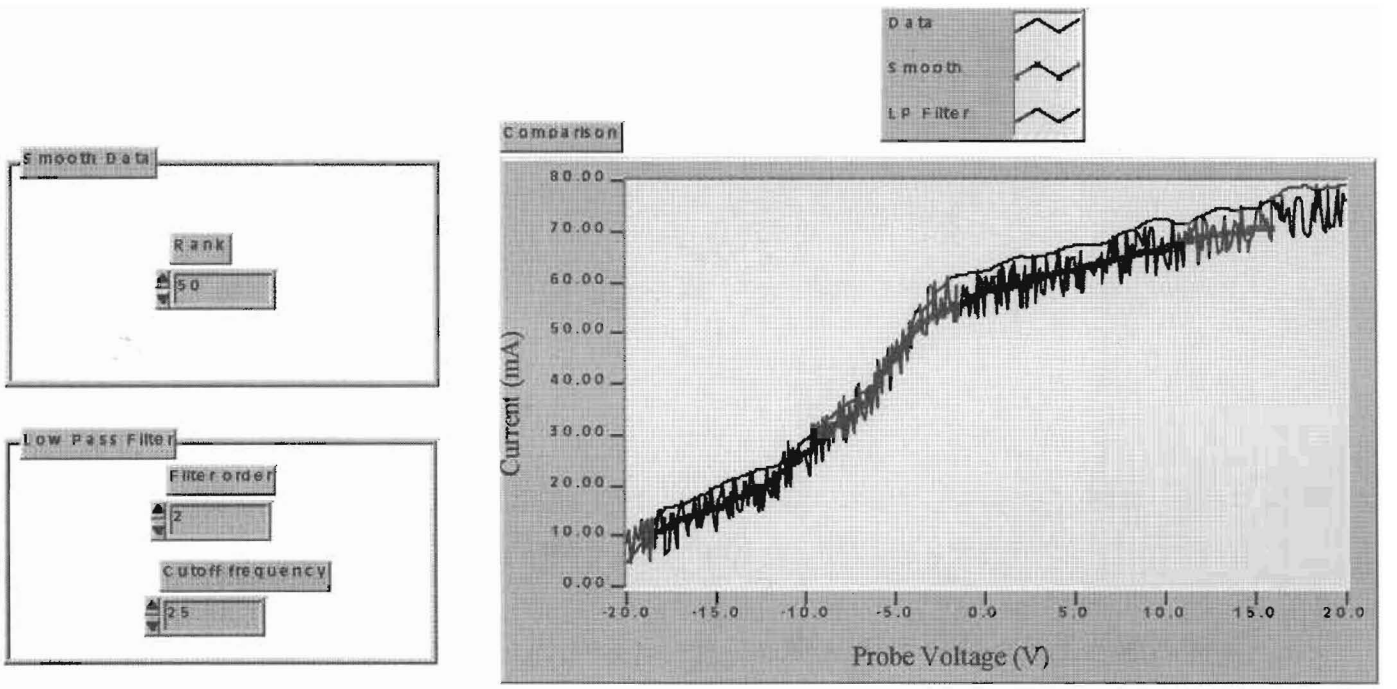

Figure 15 – Two methods of noise reduction

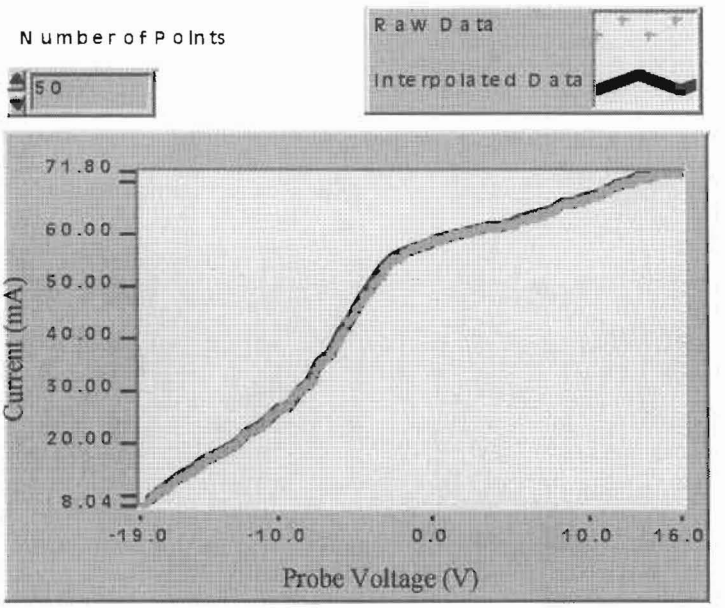

Figure 16 – This curve fit shows the Spline fit on the smoothed data.

3.2.4 Data Analysis – Spline Fit

After the noise was reduced, the LPT is fit using a Spline fit. From this fit, the user can specify the number of data points for analysis. The program automatically calculates the appropriate interval, and extracts the desired number of data points. This is beneficial in that it can add data points to better approximate the "knee" of the LPT, which occurs at the plasma space potential.

From Figure 16, the Spline fit does an excellent job fitting the curve, when we input a value of 50 data points.

3.2.5 Data Extraction

The final step in the analysis is to extract the relevant parameters. This is first done by locating the plasma space potential on the graph. Our data extraction program does this in a very sophisticated way. The second derivative of the Langmuir trace is taken and multiplied by the original curve. The derivative reveals the discontinuity and multiplying by the original function amplifies the size of the discontinuity. By finding the maximum, the program is able to determine the plasma space potential. From this, the program then extracts $I_{e\,sat}$.

Once V_s has been identified, we know at which probe voltage the function changes from the exponential region to the linear region. As discussed in Section 2.3.1, the electron temperature is proportional to the derivative of the natural log of the exponential electron current with respect to the probe bias. This curve can be seen in Figure 17, with the adjusted scaling on the x axis to end at the value of the plasma space potential. The natural log of the probe current is plotted as a function of the probe bias. The white black line represents the Langmuir trace; the solid line is the line of best fit. The reciprocal of the slope is the electron temperature, from which the density can be calculated using Equation (22). Figure 18 shows a few data runs made by changing the amount of white noise. This was done in order to show the robustness of the program.

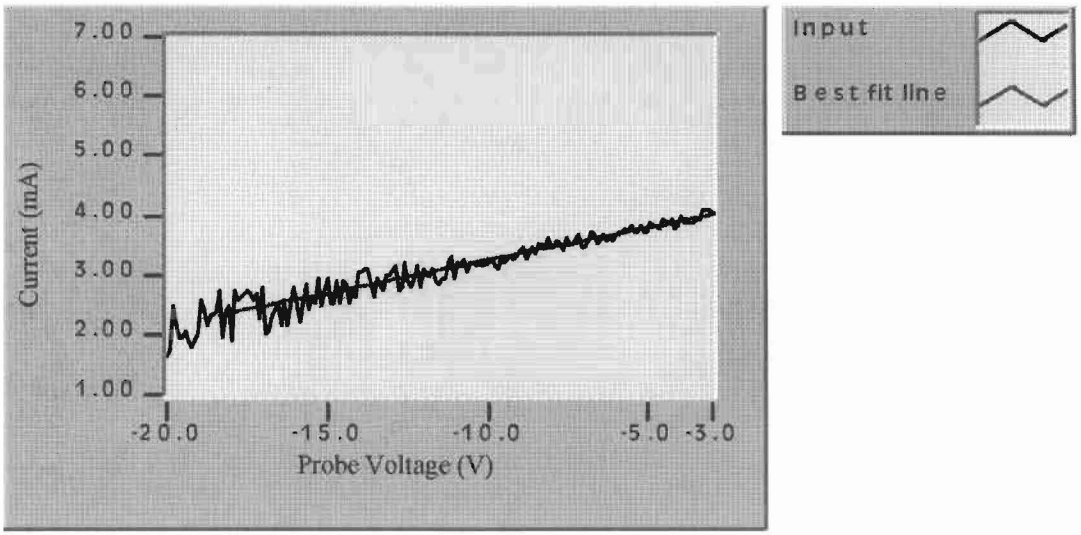

Figure 17 – Natural log of the exponential region (B), where the slope of the best curve fit line is the curvature, equal to the reciprocal of the electron temperature.

The chart in Figure 18 is based on changing the amplitude of the white noise, and examining the error from the original values of kT_e, n_e, and V_s. (The signal covers a range of about 80 mA, with the noise varying accordingly.) We can see that the % errors vary greatly – this is due in part to the increasing amount of added noise, as well as how well the smooth curve fit and the Spline fit approximate the modified curve. As the amount of noise increases, the noise reducing program has a more difficult time extracting the value of the plasma space potential, which affects the values of the other parameters.

	% Noise	% Error kT_e	% Error n_e
Trial 1	2.5	0.24	35.9
Trial 2	5	4.5	39.6
Trial 3	7.5	0.51	30.5
Trial 4	10	2.18	34.9
Trial 5	12.5	1.41	47.3
Trial 6	15	4.09	36.2
Trial 7	17.5	4.54	50.4
Trial 8	20	2.69	41.9
Trial 9	22.5	5.49	41.9
Trial 10	25	7.67	44.6
Average		3.3	40.3

Figure 18 – Table of extracted data error values

The average percent error on the electron temperature comes to 3.3%, while the error on the density comes to a surprising average of 40.3%. These percentages are satisfactory, in that the electron temperature is acceptable, and the error in the density comes from the high order of magnitude.

Chapter 4

Conclusions, Future Work, and Recommendations

While we are pleased with how well the analysis software works, the work has not ended on improving this program. The noise may be further reduced by using a Fourier Transform, instead of the current smoothing technique. Another suggestion would be to fit each region with the known functional form. The next version of this program will include a user interface, as a check on the current software analysis.

Other aspects of future work include constructing and calibrating both the Langmuir Probe and B-Dot Probe and related circuitry. Another vital part of this diagnostic system includes a circuit for optical isolation. The unit will use an octocoupler to remove any electrical connection between the device and the chamber. This is critical to the safety of the DAQ card and the computer; although the chamber is grounded, the plasma can reach a potential of 3000 V.

This project will be continued in the near future, and with the completion of the plasma device and the construction of the probes, the programs that I created in LabVIEW will be able to interpret the data and extract the relevant parameters to better model this complex system, and one step closer to understanding the physics behind this mysterious "fourth state of matter."

Bibliography

[1] Chen, Francis F. *Introduction to Plasma Physics and Controlled Fusion Vol. 1.* (Plenum Press, New York, 1984).

[2] Bova, Benjamin. The Fourth State of Matter. (St. Martin's Press, New York. 1971).

[3] Image posted on http://plasmas.org/what-are-plasmas.htm. Supplied by the *Contemporary Physics Education Project*

Gartenhaus, Solomon. *Elements of Plasma Physics*. (Holt, Rinehart, and Winston, Inc. New York, 1964).

Hayden, Douglas B. *The Application of Helicon Antennas as a Secondary Plasma Source for Ionized PVD*. University of Illinois at Urbana-Champaign.

[4] Kaufman, Harold R. Technology of Electron-Bombardment Thrusters. Advanced Electronics and Electron Physics, Vol 36. (L. Martin, ed.) Academic Press, NY, 1974. pp 265-373.

[5] Kaeppelin, V., Carrere, M., Faure, J.B. *Different Operational Regimes in a Helicon Plasma Source*. Review of Scientific Instruments. Vol. 72, Num 12. December 2001.

[6] A.J. Perry, D.Vender and R.W. Boswell, *J.Vac.Sci. Technol.* Vol 9(2), 310, (1991)

[7] Highland, Matthew. Senior Thesis – Department of Physics, Illinois Wesleyan University. 2002

[8] E.K. Bacon, "Irving Langmuir", in W.D. Miles, ed., *American Chemists and Engineers*, American Chemical Society, Washington, D.C., 1976, pp. 288-289.

[9] Image taken from http://coke.physics.ucla.edu/laptag/plasma_course.dir/langmuir.pdf, last accessed 4/25/02

Mawardi, O.K. Use *of Langmuir Probes for Low-Density Plasma Diagnostics*. Case Institute of Technology, Cleveland, Ohio. 112-120

[10] Image taken from http://www.physics.auburn.edu/~plasma/fusion/fusion_lab/cat/icrf/construction.html. last accessed 4/25/02

Smith, Hanna G. -- Smith College, Richard H. Goulding -- *Fusion Energy Division Oak Ridge National Laboratory. Construction and Calibration of a Tri-Directional Magnetic Probe for the VASIMR experiment on mini-RFTF*

Wong, A.Y. *Introduction to Experimental Plasma Physics*, UCLA report, 1977.

Information used from http://www.physics.auburn.edu/~plasma/fusion/fusion_lab/cat/icrf/construction.html (last accessed 4/25/02)

Appendix 1 A

Specifications

This appendix lists the specifications of the 6052E/6053E devices. These specifications are typical at 25 °C unless otherwise noted.

Analog Input

Input Characteristics

Number of channels

PCI-6052E ..... 16 single-ended or 8 differential (software selectable)

PCI-6053E ..... 64 single-ended or 32 differential (software selectable)

Type of ADC..... Successive approximation

Resolution ..... 16 bits, 1 in 65,536

Max sampling rate..... 333 kS/s guaranteed

Input signal ranges

Device Gain (Software Selectable)	Device Range (Software Selectable)	
	Bipolar	Unipolar
0.5	±10 V	—
1	±5 V	0 to 10 V
2	±2.5 V	0 to 5 V
5	±1 V	0 to 2 V
10	±500 mV	0 to 1 V
20	±250 mV	0 to 500 mV
50	±100 mV	0 to 200 mV
100	±50 mV	0 to 100 mV

Appendix 2

High Speed Data Acq 4a.vi
C:\WINDOWS\Desktop\Mike Mores\LabVIEW Labs\Data Log.llb\High Speed Data Acq 4a.vi
Last modified on 4/30/02 at 2:29 PM
Printed on 5/1/02 at 9:19 AM

Connector Pane

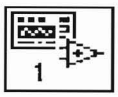

h Speed Data Acq 4

High Speed Data Acq 4a.vi
C:\WINDOWS\Desktop\Mike Mores\LabVIEW Labs\Data Log.llb\High Speed Data Acq 4a.vi
Last modified on 4/30/02 at 2:29 PM
Printed on 5/1/02 at 9:19 AM

Front Panel

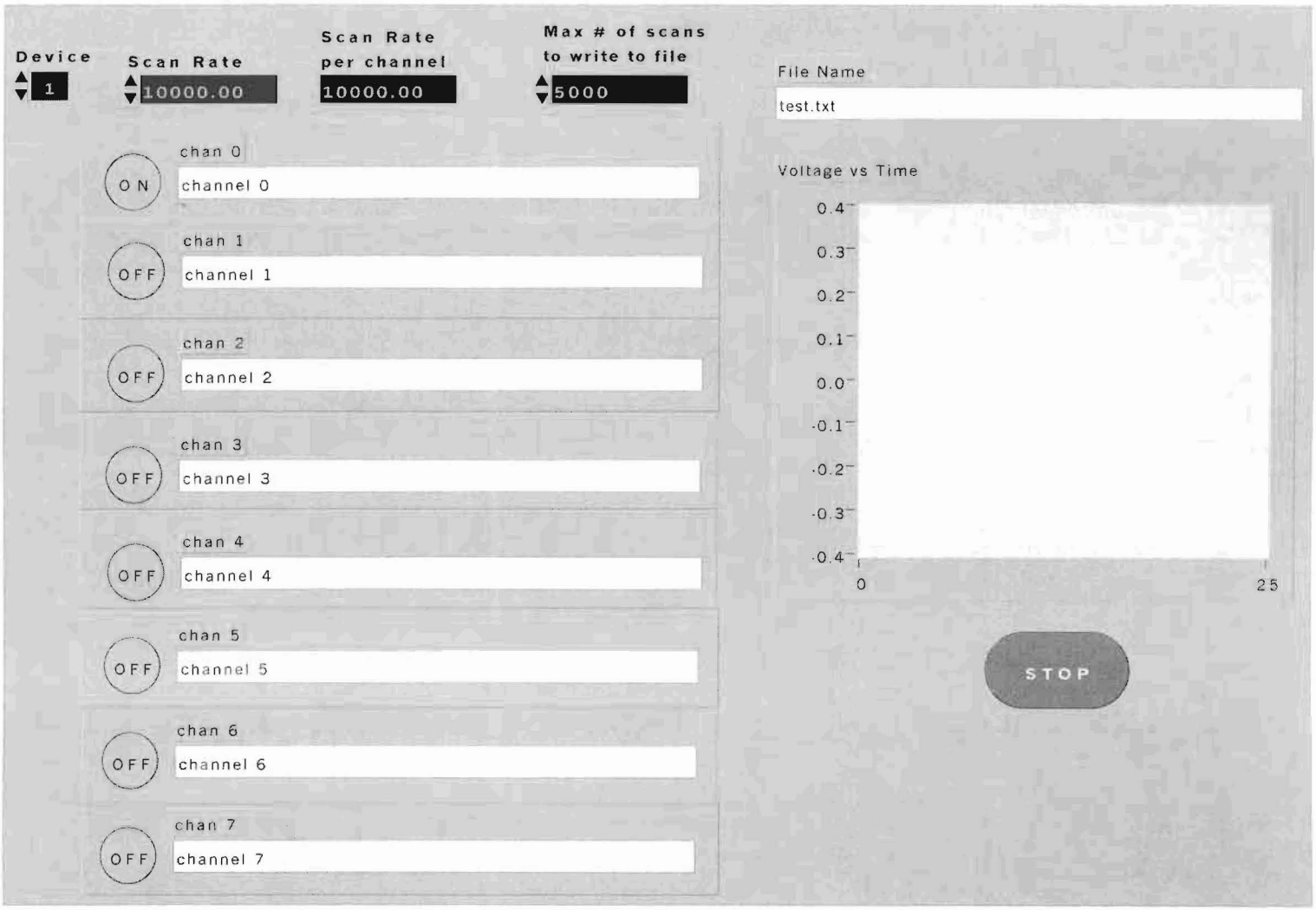

Controls and Indicators

I16 **Device**
(I16) Device: the device number you assigned to the plug-in DAQ board during configuration. This parameter defaults to 1.

I32 **Max # of scans to write to file**
(I32) Max # of scans to write to file: The maximum total number of scans you wish to stream to disk. If this is 0, data is written to disk until the stop button is pressed. Default is 500,000 scans.

SGL **Scan Rate**
(SGL) Scan Rate: The rate at which you wish to acquire and write to file. It is the number of samples per second per channel of all the listed channels. The default is 10,000 scans/sec.

TF **stop**
(TF) STOP: Stop acquiring data, and clear the board resources for the acquisition.

abc **chan 7**

abc **chan 6**

abc **chan 5**

abc **chan 4**

abc **chan 3**

abc **chan 2**

abc **chan 1**

abc **chan 0**

abc **File Name**

TF **bool 0**

TF **bool1**

TF **bool 2**

TF **bool 3**

TF **bool 4**

TF **bool 5**

TF **bool 6**

TF **bool 7**

[SGL]

SGL **Scan Rate**
per channel
(SGL) Scan Rate: The rate at which you wish to acquire and write to file. It is the number of samples per second per channel of all the listed channels. The default is 10,000 scans/sec.

Block Diagram

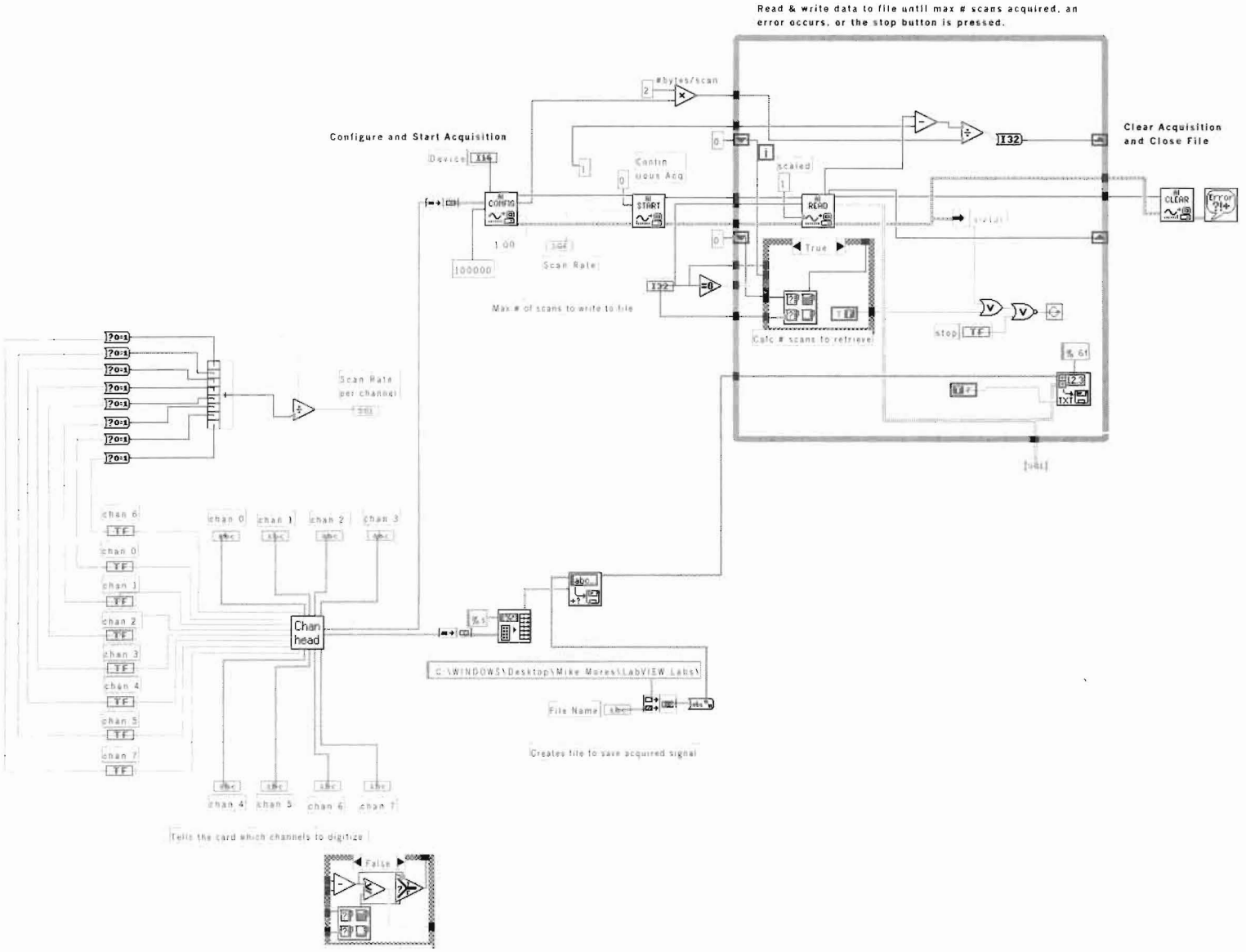

High Speed Data Acq 4a.vi
C:\WINDOWS\Desktop\Mike Mores\LabVIEW Labs\Data Log.llb\High Speed Data Acq 4a.vi
Last modified on 4/30/02 at 2:29 PM
Printed on 5/1/02 at 9:19 AM

List of SubVIs

General Error Handler.vi
C:\PROGRAM FILES\NATIONAL INSTRUMENTS\LABVIEW\vi.lib\Utility\error.llb\General Error

AI Clear.vi
C:\PROGRAM FILES\NATIONAL INSTRUMENTS\LABVIEW\vi.lib\DAQ\AI.LLB\AI Clear.vi

AI Config.vi
C:\PROGRAM FILES\NATIONAL INSTRUMENTS\LABVIEW\vi.lib\DAQ\AI.LLB\AI Config.vi

AI Start.vi
C:\PROGRAM FILES\NATIONAL INSTRUMENTS\LABVIEW\vi.lib\DAQ\AI.LLB\AI Start.vi

AI Read.vi
C:\PROGRAM FILES\NATIONAL INSTRUMENTS\LABVIEW\vi.lib\DAQ\AI.LLB\AI Read.vi

Write To Spreadsheet File.vi
C:\PROGRAM FILES\NATIONAL INSTRUMENTS\LABVIEW\vi.lib\Utility\file.llb\Write To Spreadsheet File.vi

Write Characters To File.vi
C:\PROGRAM FILES\NATIONAL INSTRUMENTS\LABVIEW\vi.lib\Utility\file.llb\Write Characters To

Channel Description
C:\WINDOWS\Desktop\Mike Mores\LabVIEW Labs\Data Log.llb\Channel Description

LPT Analysis
C:\WINDOWS\Desktop\Mike Mores\LabVIEW Labs\Langmuir.llb\LPT Analysis
Last modified on 5/1/02 at 1:12 AM
Printed on 5/1/02 at 9:27 AM

Connector Pane

PT Analysi

Front Panel

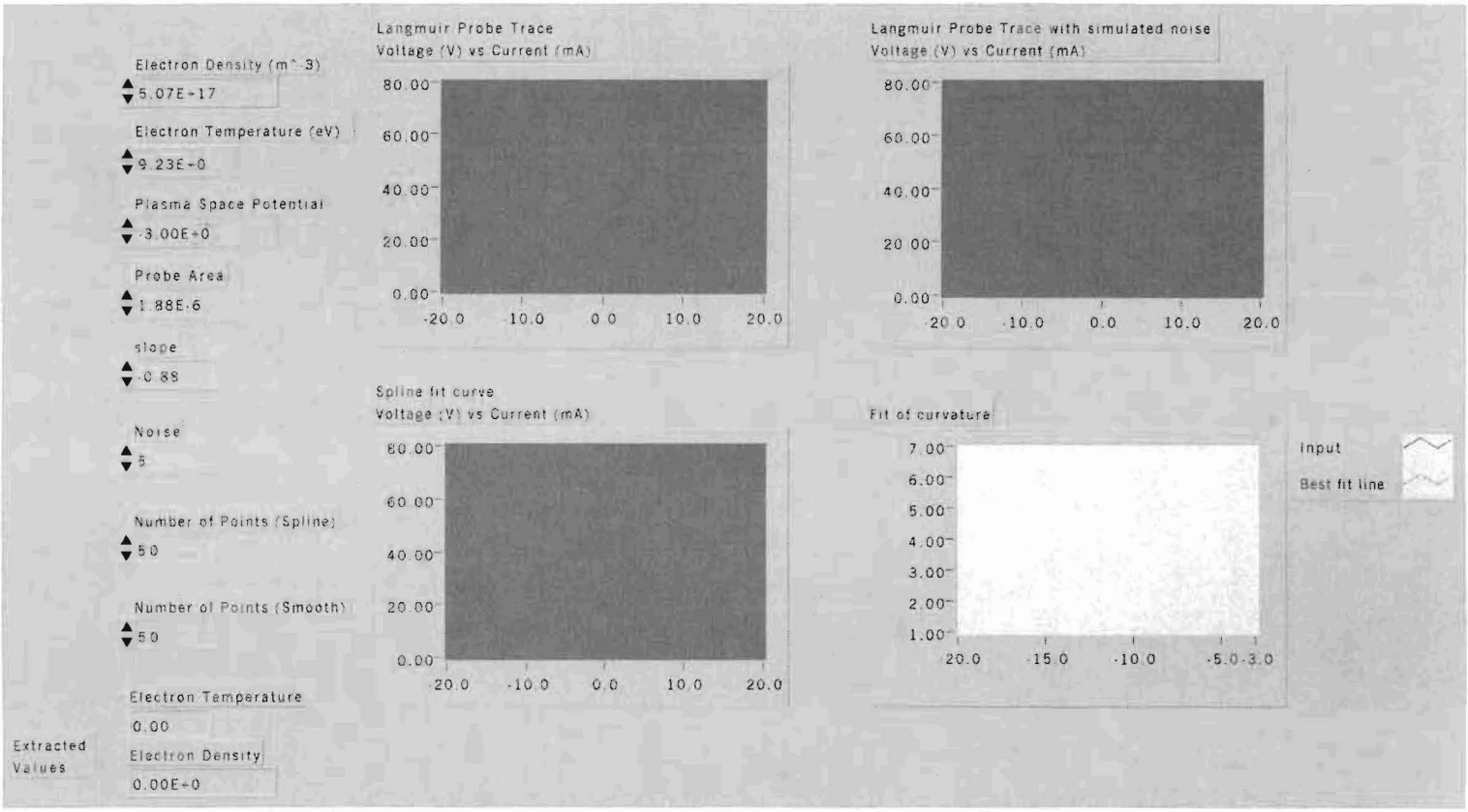
Electron Density (m^-3)
5.07E+17
Electron Temperature (eV)
9.23E+0
Plasma Space Potential
3.00E+0
Probe Area
1.88E-6
slope
-0.88
Noise
5
Number of Points (Spline)
50
Number of Points (Smooth)
50
Electron Temperature
0.00
Electron Density
0.00E+0
Extracted Values
Langmuir Probe Trace
Voltage (V) vs Current (mA)
80.00
60.00
40.00
20.00
0.00
-20.0
-10.0
0.0
10.0
20.0
Langmuir Probe Trace with simulated noise
Voltage (V) vs Current (mA)
Spline fit curve
Voltage (V) vs Current (mA)
Fit of curvature
7.00
6.00
5.00
4.00
3.00
2.00
1.00
-20.0
-15.0
-10.0
-5.0
-3.0
Input
Best fit line

Controls and Indicators

DBL **Probe Area**

DBL **Electron Density (m^-3)**

DBL **Electron Temperature (eV)**

DBL **slope**

DBL **Plasma Space Potential**

I16 **Number of Points (Spline)**

I8 **Noise**

I16 **Number of Points (Smooth)**

Langmuir Probe Trace
Voltage (V) vs Current (mA)

Langmuir Probe Trace with simulated noise
Voltage (V) vs Current (mA)

Spline fit curve
Voltage (V) vs Current (mA)

Fit of curvature

DBL **Electron Temperature**

DBL **Electron Density**

Block Diagram

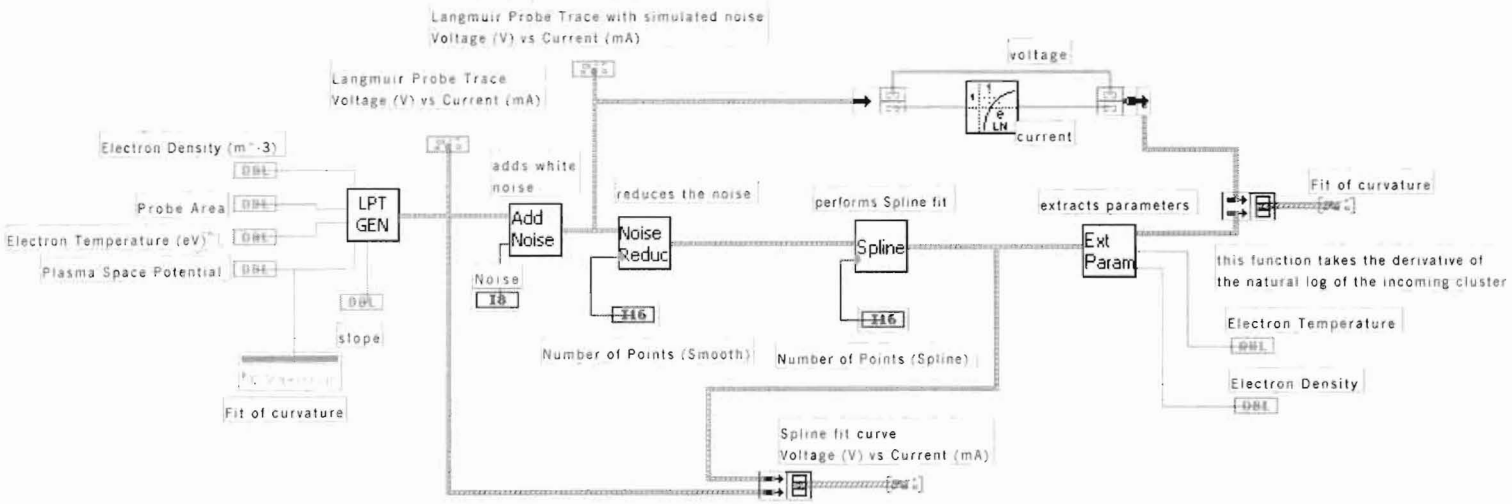

List of SubVIs

LPT Generator
C:\WINDOWS\Desktop\Mike Mores\LabVIEW Labs\Langmuir.llb\LPT Generator

Noise Adder
C:\WINDOWS\Desktop\Mike Mores\LabVIEW Labs\Langmuir.llb\Noise Adder

Spline Fit
C:\WINDOWS\Desktop\Mike Mores\LabVIEW Labs\Langmuir.llb\Spline Fit

Extract_Parameters.vi
C:\WINDOWS\Desktop\Mike Mores\LabVIEW Labs\Langmuir.llb\Extract_Parameters.vi

noise reduction.vi
C:\WINDOWS\Desktop\Mike Mores\LabVIEW Labs\Langmuir.llb\noise reduction.vi

LPT Generator
C:\WINDOWS\Desktop\Mike Mores\LabVIEW Labs\Langmuir.llb\LPT Generator
Last modified on 5/1/02 at 1:08 AM
Printed on 5/1/02 at 9:27 AM

Connector Pane

LPT Generator

Front Panel

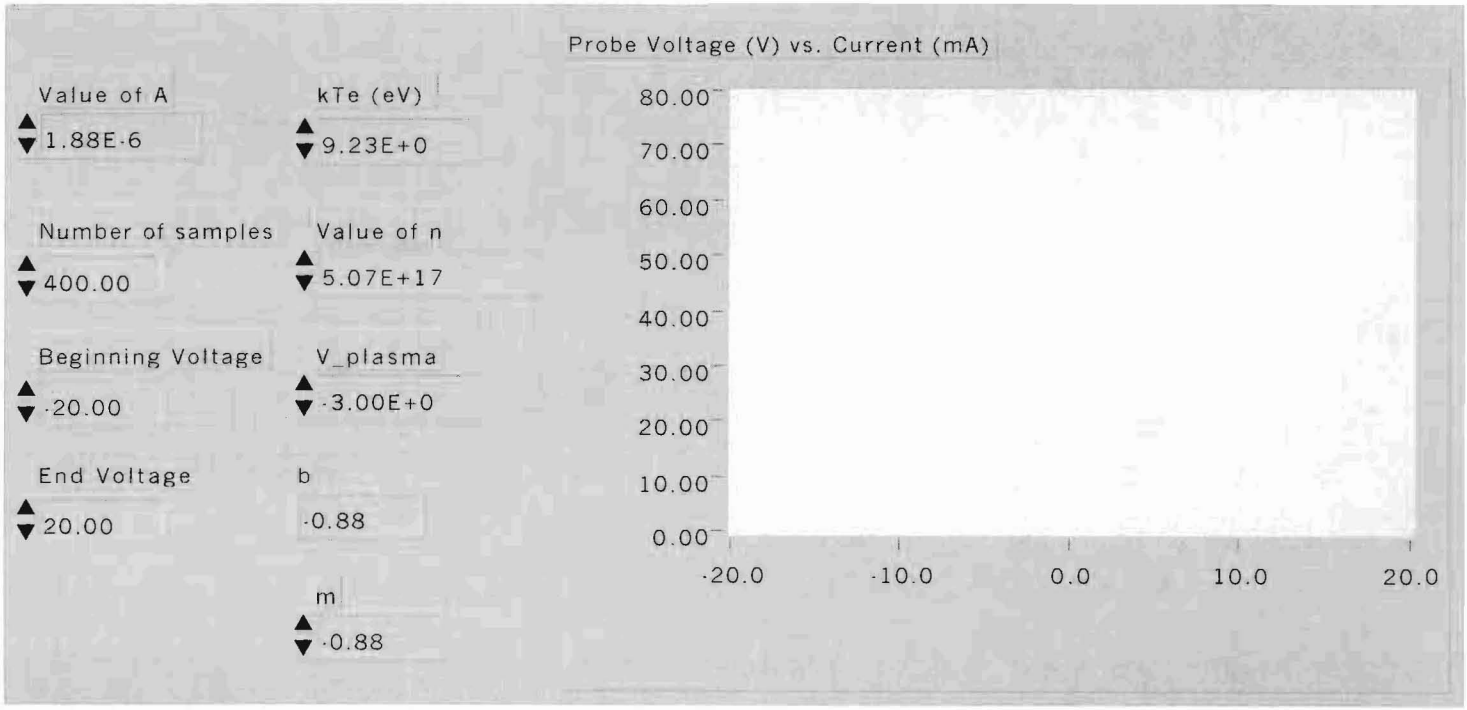
Value of A
1.88E-6
kTe (eV)
9.23E+0
Number of samples
400.00
Value of n
5.07E+17
Beginning Voltage
-20.00
V_plasma
-3.00E+0
End Voltage
20.00
b
-0.88
m
-0.88
Probe Voltage (V) vs. Current (mA)
80.00
70.00
60.00
50.00
40.00
30.00
20.00
10.00
0.00
-20.0
-10.0
0.0
10.0
20.0

Controls and Indicators

- DBL **Value of A**
- DBL **Value of n**
- DBL **kTe (eV)**
- DBL **m**
- DBL **V_plasma**
- DBL **Beginning Voltage**
- DBL **End Voltage**
- DBL **Number of samples**
-  **Probe Voltage (V) vs. Current (mA)**
- DBL **b**

Block Diagram

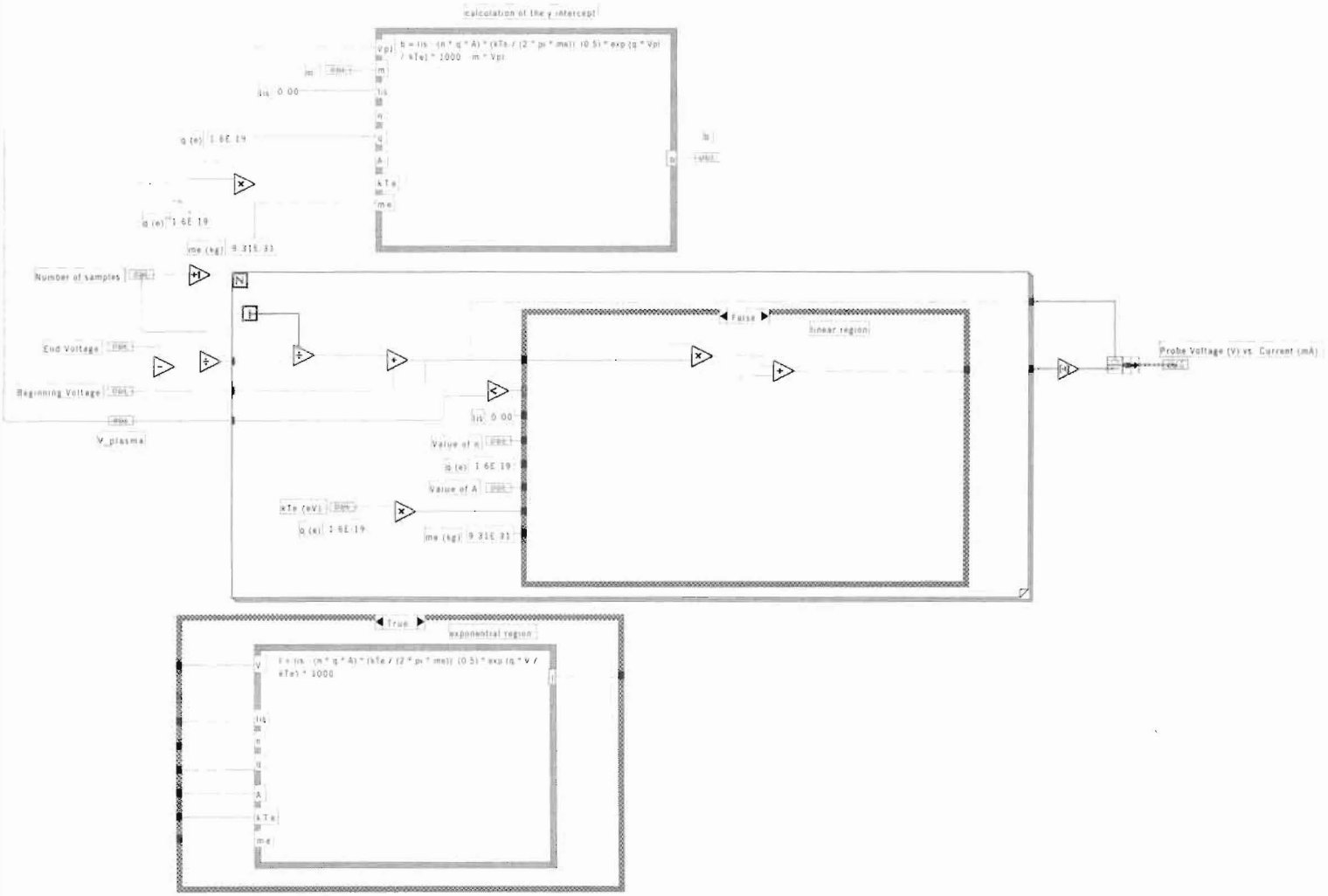

Noise Adder
C:\WINDOWS\Desktop\Mike Mores\LabVIEW Labs\Langmuir.llb\Noise Adder
Last modified on 5/1/02 at 12:41 AM
Printed on 5/1/02 at 9:28 AM

Connector Pane

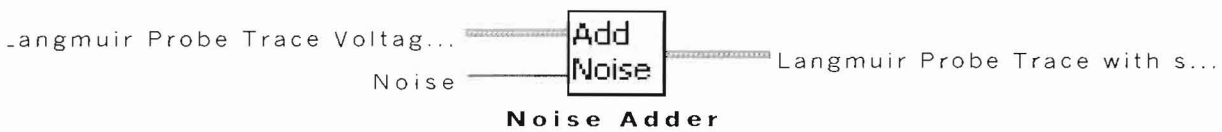

Add Noise

Front Panel

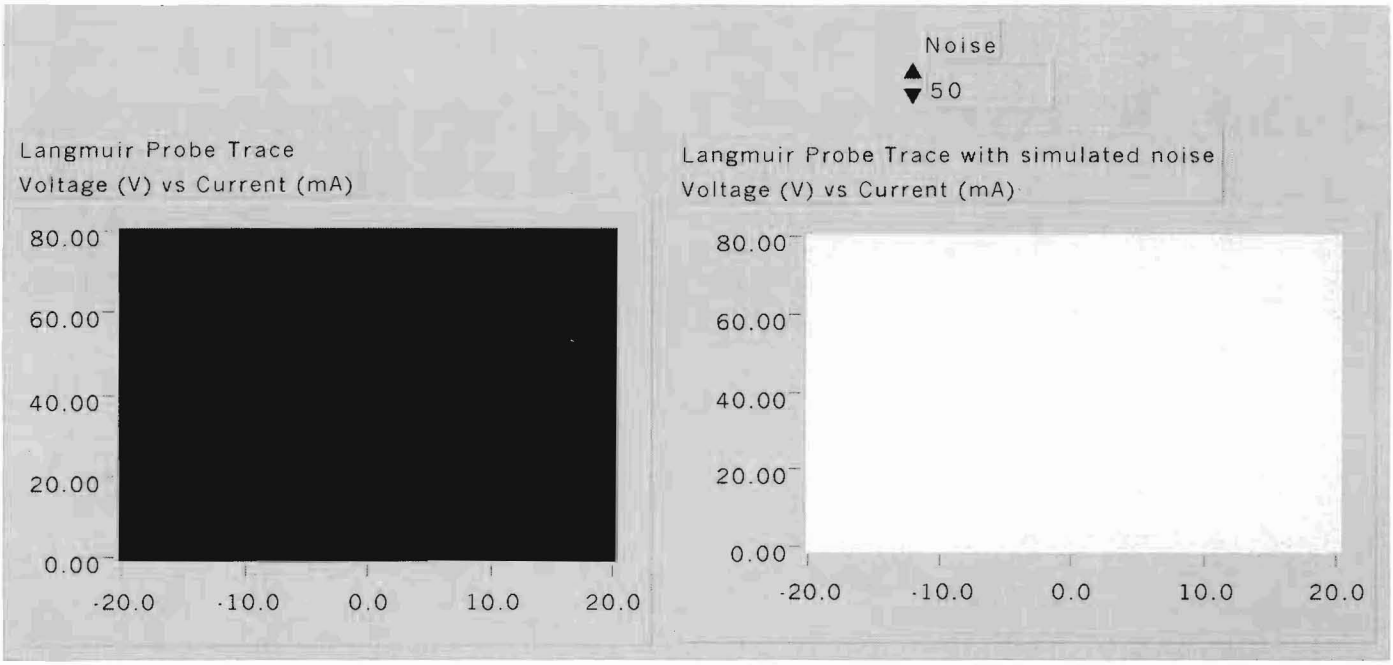

Controls and Indicators

Noise

Langmuir Probe Trace
Voltage (V) vs Current (mA)

Langmuir Probe Trace with simulated noise
Voltage (V) vs Current (mA)

Noise Adder
C:\WINDOWS\Desktop\Mike Mores\LabVIEW Labs\Langmuir.llb\Noise Adder
Last modified on 5/1/02 at 12:41 AM
Printed on 5/1/02 at 9:28 AM

Block Diagram

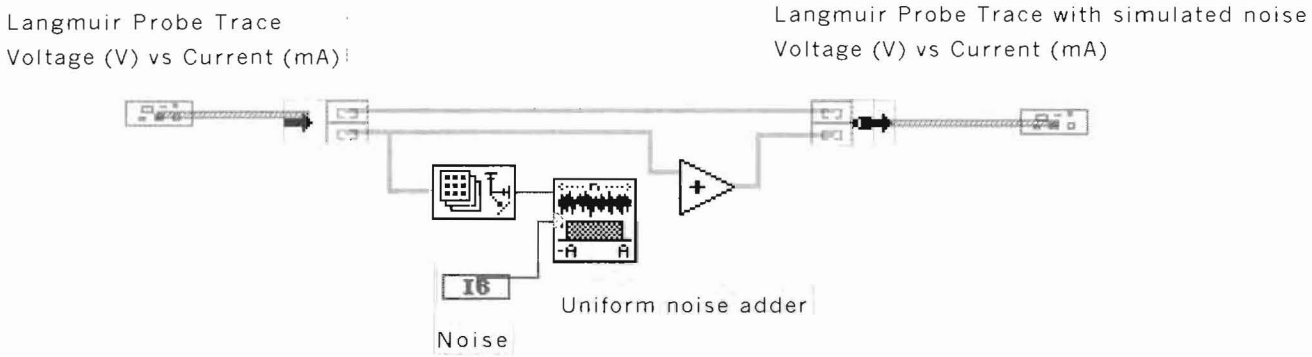

noise reduction.vi
C:\WINDOWS\Desktop\Mike Mores\LabVIEW Labs\Langmuir.llb\noise reduction.vi
Last modified on 5/1/02 at 1:09 AM
Printed on 5/1/02 at 9:33 AM

Connector Pane

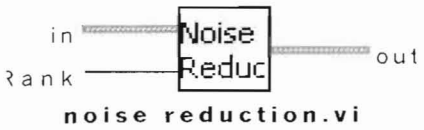

Front Panel

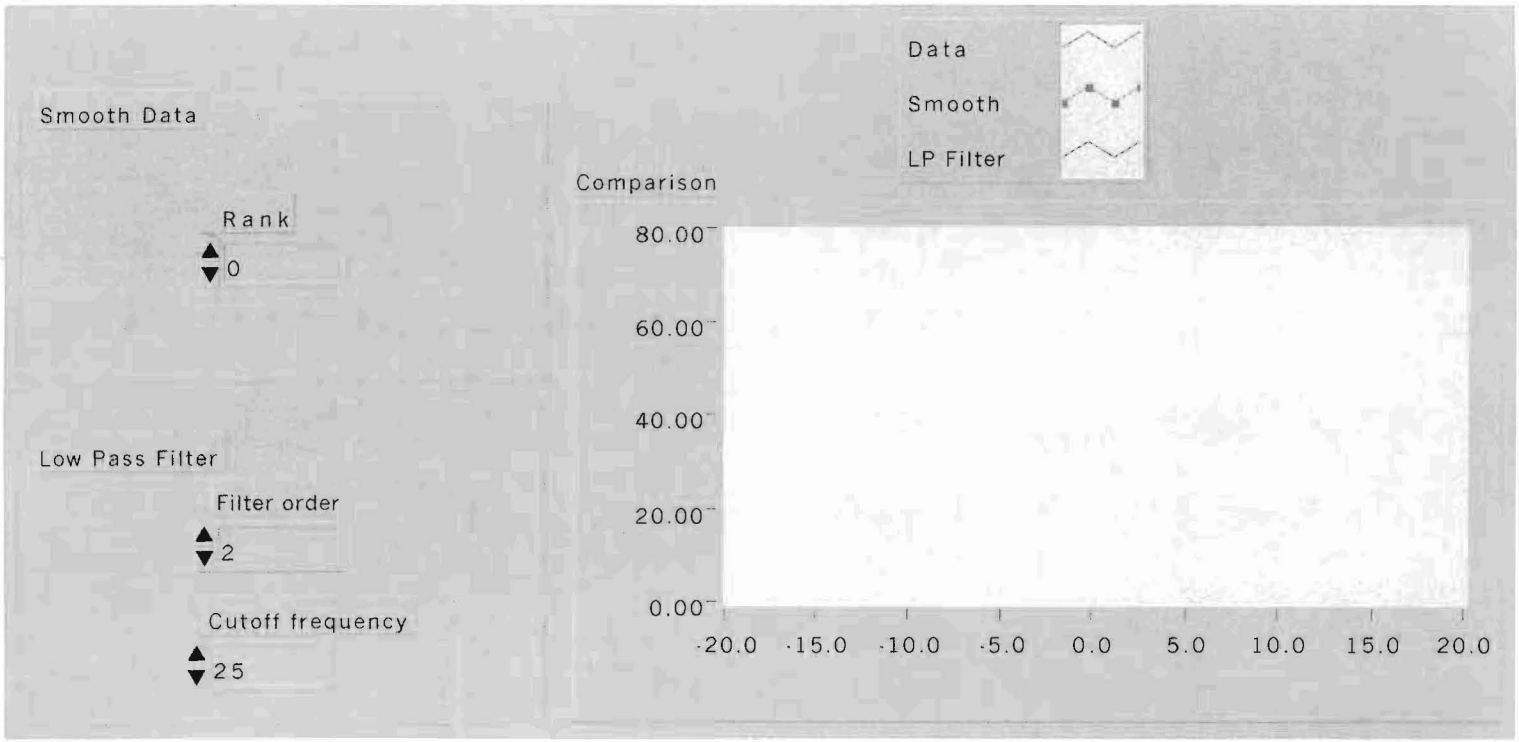
Smooth Data
Rank
0
Low Pass Filter
Filter order
2
Cutoff frequency
25
Comparison
Data
Smooth
LP Filter
80.00
60.00
40.00
20.00
0.00
-20.0
-15.0
-10.0
-5.0
0.0
5.0
10.0
15.0
20.0

Controls and Indicators

- in
- Rank
- subset
- Filter order
- Cutoff frequency
- out
- Comparison
- [DBL]

Block Diagram

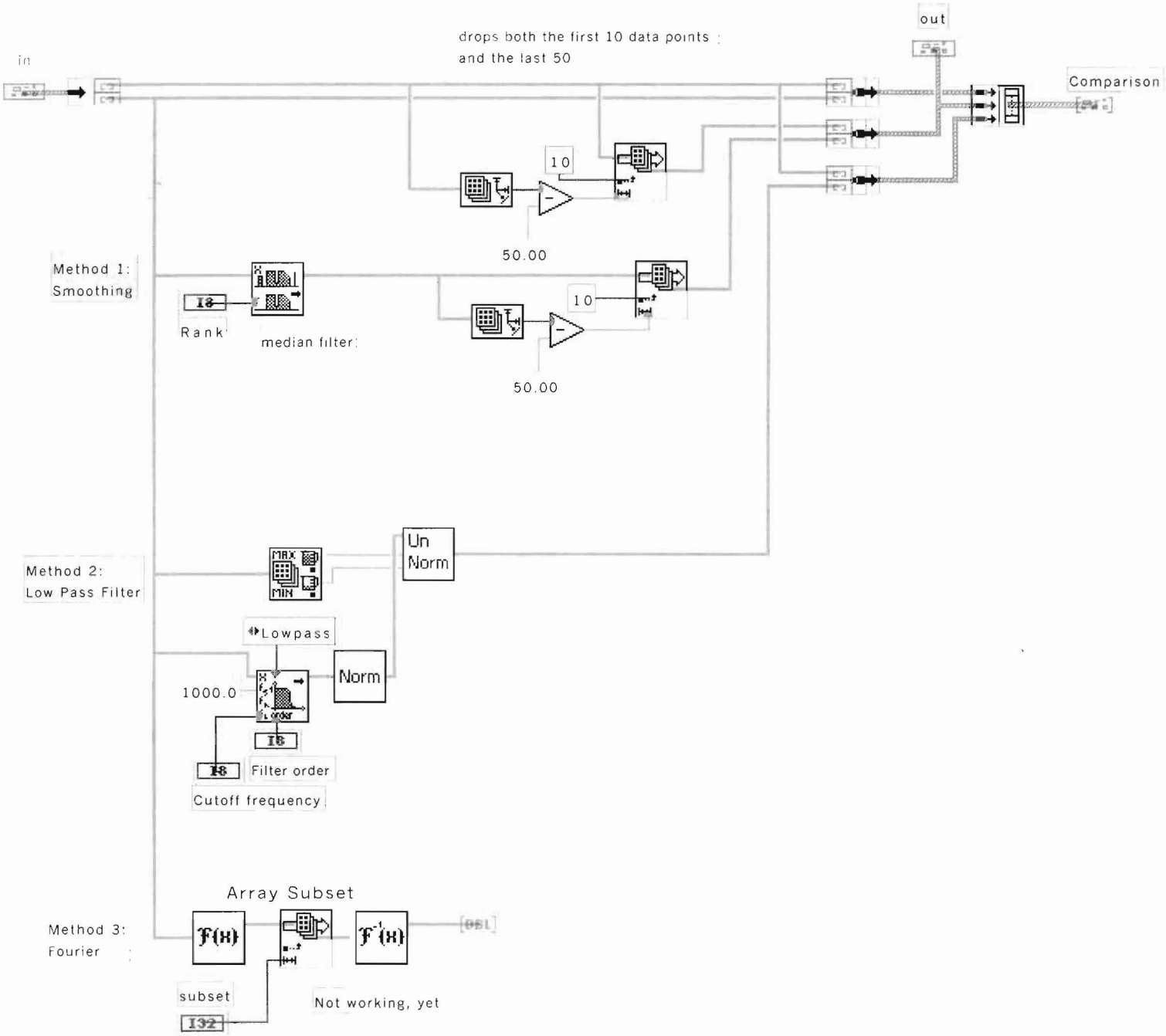

noise reduction.vi
C:\WINDOWS\Desktop\Mike Mores\LabVIEW Labs\Langmuir.llb\noise reduction.vi
Last modified on 5/1/02 at 1:09 AM
Printed on 5/1/02 at 9:33 AM

List of SubVIs

Median Filter.vi
C:\PROGRAM FILES\NATIONAL INSTRUMENTS\LABVIEW\vi.lib\Analysis\3filter.llb\Median Filter.vi

Real FFT.vi
C:\PROGRAM FILES\NATIONAL INSTRUMENTS\LABVIEW\vi.lib\Analysis\2dsp.llb\Real FFT.vi

Inverse Real FFT.vi
C:\PROGRAM FILES\NATIONAL INSTRUMENTS\LABVIEW\vi.lib\Analysis\2dsp.llb\Inverse Real

Butterworth Filter.vi
C:\PROGRAM FILES\NATIONAL INSTRUMENTS\LABVIEW\vi.lib\Analysis\3filter.llb\Butterworth

UNnormalize data.vi
C:\WINDOWS\Desktop\Mike Mores\LabVIEW Labs\Langmuir.llb\UNnormalize data.vi

normalize data.vi
C:\WINDOWS\Desktop\Mike Mores\LabVIEW Labs\Langmuir.llb\normalize data.vi

normalize data.vi
C:\WINDOWS\Desktop\Mike Mores\LabVIEW Labs\Langmuir.llb\normalize data.vi
Last modified on 5/1/02 at 12:45 AM
Printed on 5/1/02 at 9:33 AM

Connector Pane

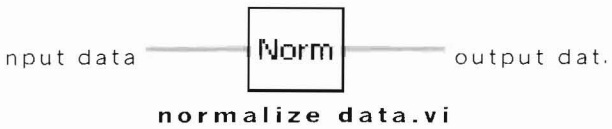

normalize data.vi

This vi takes input data and normalized it. It determines the values needed for normalization

normalize data.vi
C:\WINDOWS\Desktop\Mike Mores\LabVIEW Labs\Langmuir.llb\normalize data.vi
Last modified on 5/1/02 at 12:45 AM
Printed on 5/1/02 at 9:33 AM

Front Panel

Norm

normalize data.vi
C:\WINDOWS\Desktop\Mike Mores\LabVIEW Labs\Langmuir.llb\normalize data.vi
Last modified on 5/1/02 at 12:45 AM
Printed on 5/1/02 at 9:33 AM

Controls and Indicators

DBL **input data**

DBL

DBL **output data**

DBL

normalize data.vi
C:\WINDOWS\Desktop\Mike Mores\LabVIEW Labs\Langmuir.llb\normalize data.vi
Last modified on 5/1/02 at 12:45 AM
Printed on 5/1/02 at 9:33 AM

Block Diagram

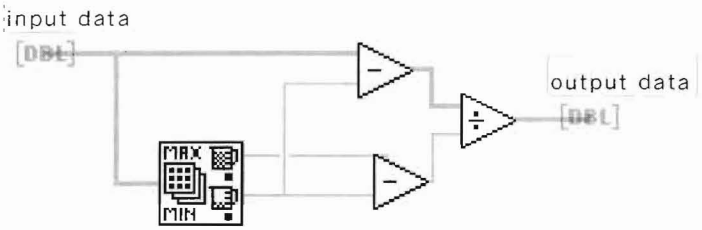

UNnormalize data.vi
C:\WINDOWS\Desktop\Mike Mores\LabVIEW Labs\Langmuir.llb\UNnormalize data.vi
Last modified on 5/1/02 at 12:46 AM
Printed on 5/1/02 at 9:33 AM

Connector Pane

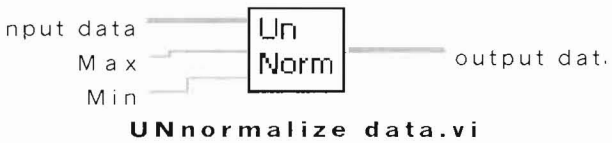

UNnormalize data.vi

This vi takes input data and unnormalized it, based on user define min and max values.

UNnormalize data.vi
C:\WINDOWS\Desktop\Mike Mores\LabVIEW Labs\Langmuir.llb\UNnormalize data.vi
Last modified on 5/1/02 at 12:46 AM
Printed on 5/1/02 at 9:33 AM

Front Panel

UNnormalize data.vi
C:\WINDOWS\Desktop\Mike Mores\LabVIEW Labs\Langmuir.llb\UNnormalize data.vi
Last modified on 5/1/02 at 12:46 AM
Printed on 5/1/02 at 9:33 AM

Controls and Indicators

[DBL] **input data**

[DBL]

[DBL] **Min**

[DBL] **Max**

[DBL] **output data**

[DBL]

UNnormalize data.vi
C:\WINDOWS\Desktop\Mike Mores\LabVIEW Labs\Langmuir.llb\UNnormalize data.vi
Last modified on 5/1/02 at 12:46 AM
Printed on 5/1/02 at 9:33 AM

Block Diagram

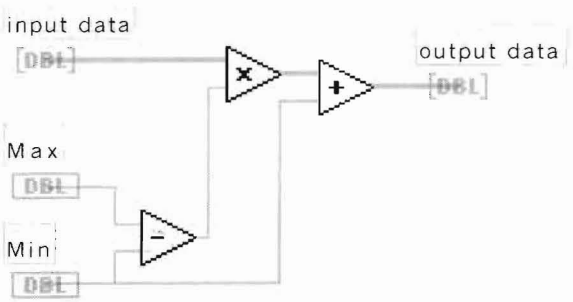

Connector Pane

Spline Fit

This example demonstrates the use of various interpolation VIs including:

- Linear Interpolation
- Polynomial Interpolation
- Spline Interpolation
- Rational Interpolation

Spline Fit
C:\WINDOWS\Desktop\Mike Mores\LabVIEW Labs\Langmuir.llb\Spline Fit
Last modified on 5/1/02 at 1:10 AM
Printed on 5/1/02 at 9:34 AM

Front Panel

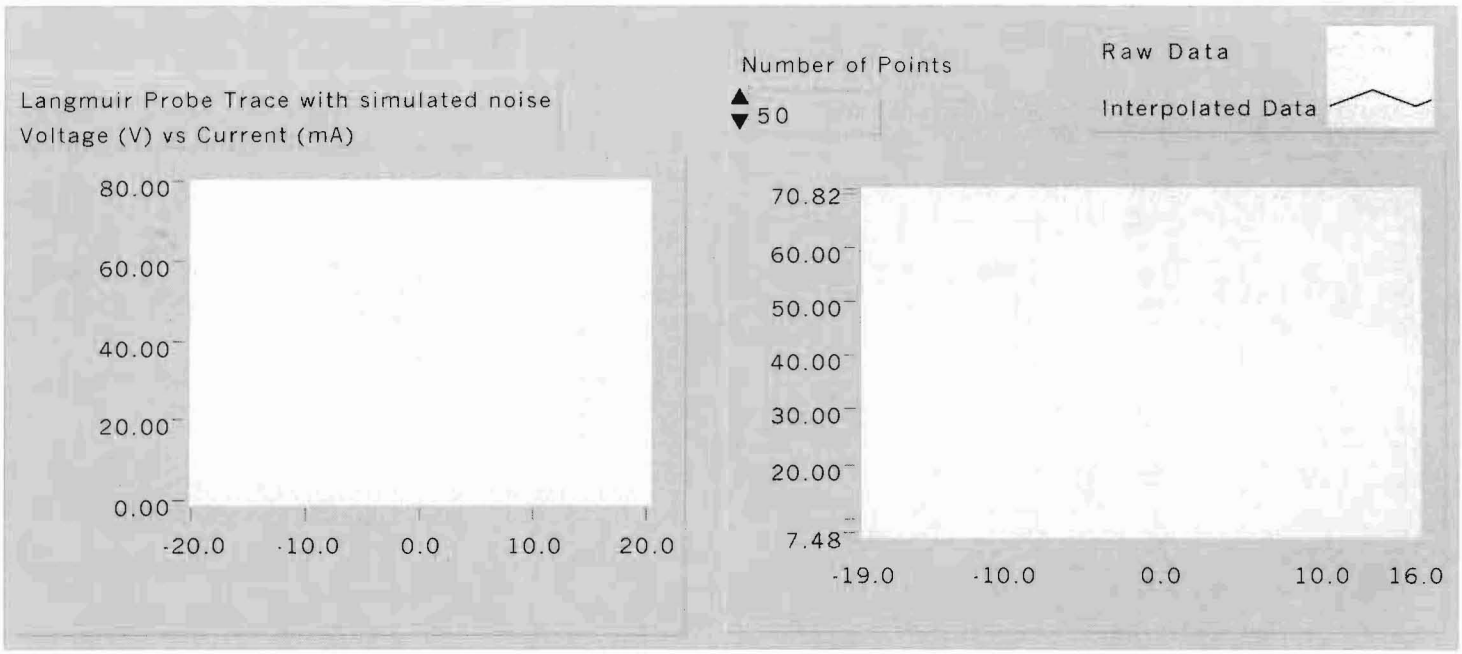

Spline Fit
C:\WINDOWS\Desktop\Mike Mores\LabVIEW Labs\Langmuir.llb\Spline Fit
Last modified on 5/1/02 at 1:10 AM
Printed on 5/1/02 at 9:33 AM

Controls and Indicators

I32 **Number of Points**

Langmuir Probe Trace with simulated noise
Voltage (V) vs Current (mA)

Raw Data and Interpolated Data

Curve

[DBL]

DBL

[DBL]

DBL **interpolation value**

Spline Fit
C:\WINDOWS\Desktop\Mike Mores\LabVIEW Labs\Langmuir.llb\Spline Fit
Last modified on 5/1/02 at 1:10 AM
Printed on 5/1/02 at 9:33 AM

Block Diagram

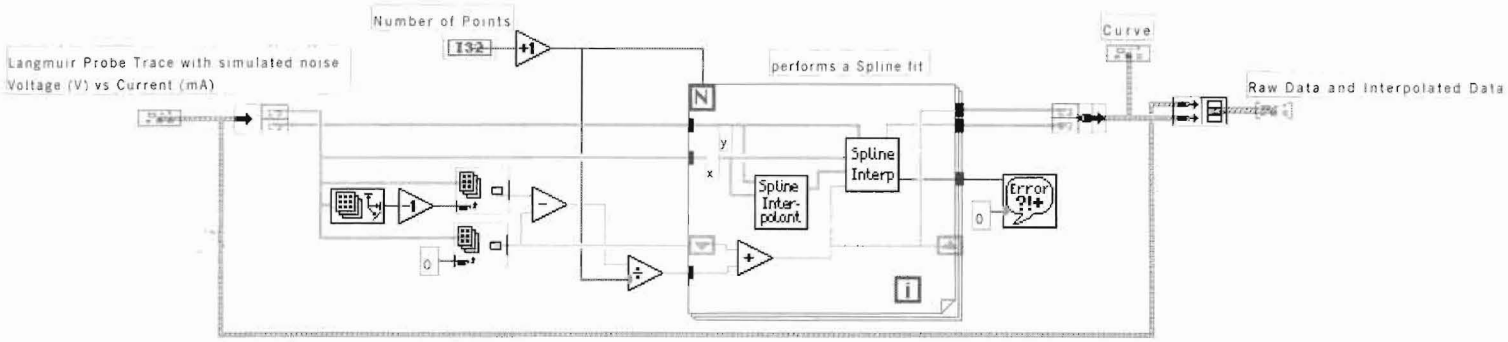

Extract_Parameters.vi
C:\WINDOWS\Desktop\Mike Mores\LabVIEW Labs\Langmuir.llb\Extract_Parameters.vi
Last modified on 5/1/02 at 1:11 AM
Printed on 5/1/02 at 9:34 AM

Connector Pane

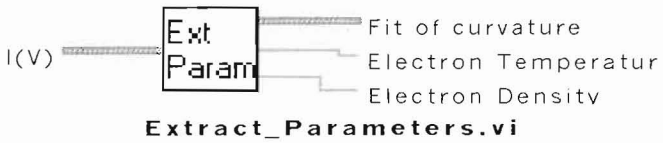

Extract_Parameters.vi
C:\WINDOWS\Desktop\Mike Mores\LabVIEW Labs\Langmuir.llb\Extract_Parameters.vi
Last modified on 5/1/02 at 1:11 AM
Printed on 5/1/02 at 9:34 AM

Front Panel

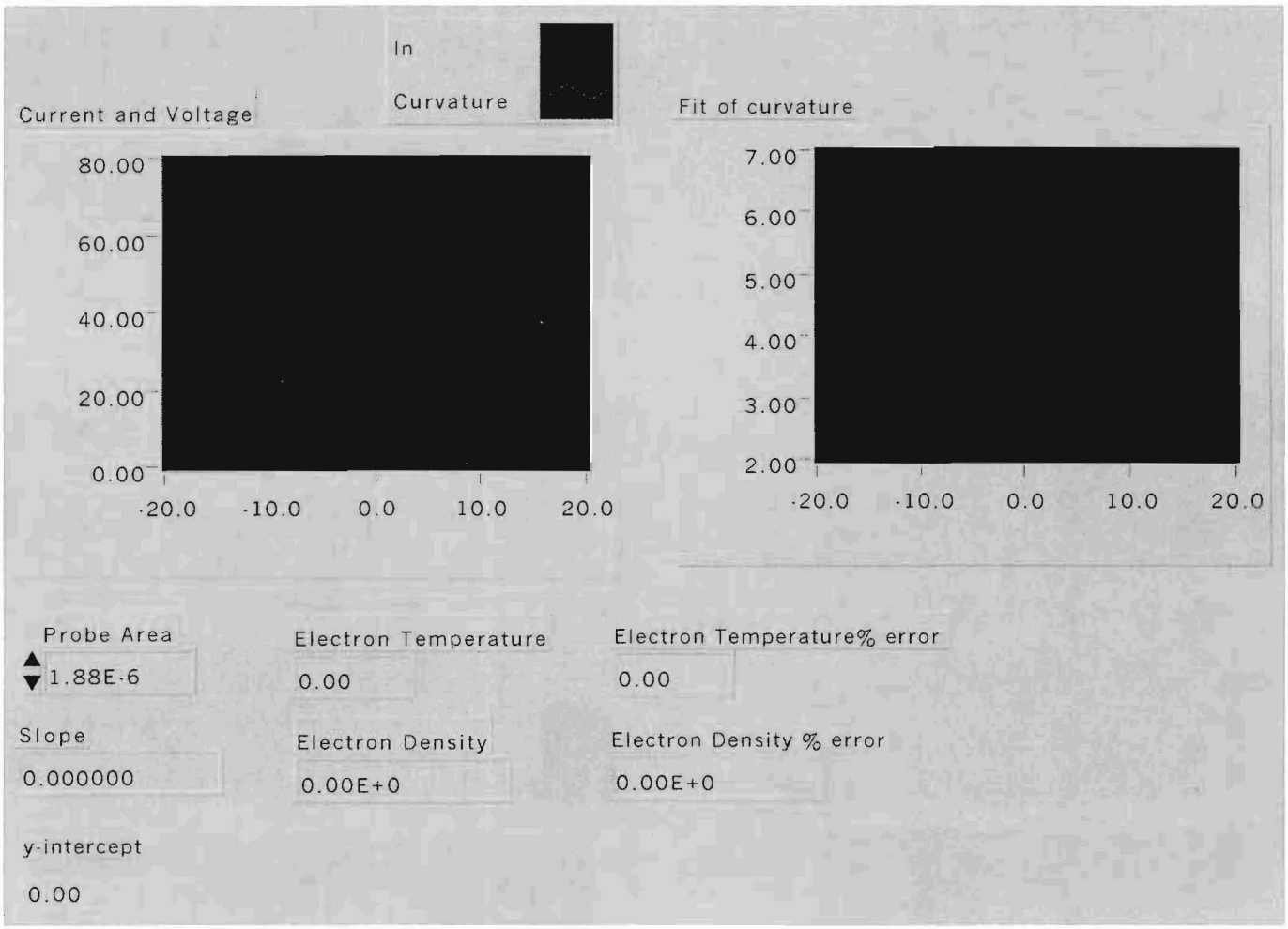

Extract_Parameters.vi
C:\WINDOWS\Desktop\Mike Mores\LabVIEW Labs\Langmuir.llb\Extract_Parameters.vi
Last modified on 5/1/02 at 1:11 AM
Printed on 5/1/02 at 9:34 AM

Controls and Indicators

- I(V)
  - [DBL]
    - DBL
  - [DBL]
    - DBL y
- DBL Probe Area
- DBL Slope
- Current and Voltage
- DBL y-intercept
- Fit of curvature
- DBL Electron Temperature
- DBL Electron Density
- DBL Electron Temperature% error
- DBL Electron Density % error

Extract_Parameters.vi
C:\WINDOWS\Desktop\Mike Mores\LabVIEW Labs\Langmuir.llb\Extract_Parameters.vi
Last modified on 5/1/02 at 1:11 AM
Printed on 5/1/02 at 9:34 AM

Block Diagram